

Electroweak Phase Transition in the $\mu\nu$ SSM

Daniel J. H. Chung^{1,2,*} and Andrew J. Long^{1,†}

¹ *University of Wisconsin-Madison, Department of Physics
1150 University Avenue, Madison, WI 53706, USA*

² *School of Physics, Korea Institute for Advanced Study, 207-43,
Cheongnyangni2-dong, Dongdaemun-gu, Seoul 130-722, Korea*

(Dated: 4/06/10)

An extension of the MSSM called the $\mu\nu$ SSM does not allow a conventional thermal leptogenesis scenario because of the low scale seesaw that it utilizes. Hence, we investigate the possibility of electroweak baryogenesis. Specifically, we identify a parameter region for which the electroweak phase transition is sufficiently strongly first order to realize electroweak baryogenesis. In addition to transitions that are similar to those in the NMSSM, we find a novel class of phase transitions in which there is a rotation in the singlet vector space.

1. INTRODUCTION

An extension of the MSSM called the $\mu\nu$ SSM [2] is a model similar to the NMSSM [1] (with the usual \mathbb{Z}_3 charge assignment) except that the singlet whose vacuum expectation value (VEV) gives rise to the μ term also serves the role of a right-handed neutrino, thereby violating R-parity. Because the VEV generates the μ -term and the right handed neutrino mass, the right-handed neutrino masses are of order TeV, leading to a low scale type I seesaw. Given the absence of high scale seesaw, thermal leptogenesis is difficult in the $\mu\nu$ SSM. Hence, it is interesting to consider whether or not electroweak baryogenesis (EWBG) [4] can occur in this class of models. One of the most stringent constraints of EWBG on the $\mu\nu$ SSM is the requirement of a sufficiently strongly first order phase transition (SFOPT) such that the created baryons are not washed out [5].

Because the $\mu\nu$ SSM contains 3 singlet chiral superfields (right handed neutrinos), mainly motivated by generality, standard model generation replication pattern, and phenomenological convenience [2, 3], there is a “larger” SFOPT parameter space for EWBG when compared to the NMSSM. More precisely, there can be SFOPT where the singlet VEVs rotate in the singlet vector space during the electroweak phase transition. The price paid for this is a more complicated global minimum analysis at both finite and zero temperatures. The aim of this paper is not to uncover the most general parameter space consistent with EWBG, but is to simply give a couple of parametric regions to show the existence of possibilities.

Depending on the path of the phase transition, the exact $\mu\nu$ SSM parametric dependence of the phase transition strength $v(T_c)/T_c$ is complicated. Nonetheless, we find that it is typically true that to achieve SFOPT, the parameters are close to satisfying the following

*Electronic address: danielchung@wisc.edu

†Electronic address: ajlong@wisc.edu

condition:

$$\frac{E_{\text{eff}}}{\lambda_{\text{eff}}v(0)} \approx \frac{1}{2} \quad (1)$$

where E_{eff} is the effective cubic coupling, λ_{eff} is the effective quartic coupling, and $v(0)$ is the magnitude of the scalar field space VEV (including both the Higgs and singlets) at zero temperature. Physically, this corresponds to the parametric region where the critical temperature T_c is small compared to $v(0)$ during the electroweak phase transition. In the examples provided in this paper, whether or not the SFOPT proceeds from the origin, the leading non-vanishing value of E_{eff} in the $\mu\nu$ SMS arises from the soft terms

$$\sum_i^3 \left[-a_\lambda H_1 H_2 \tilde{\nu}_i^c + \frac{1}{3} a_\kappa (\tilde{\nu}_i^c)^3 + \text{h.c.} \right] \quad (2)$$

where $\tilde{\nu}_i^c$ are singlet fields. The dimensionful coupling a_λ is distinguished from a_κ in that a_λ also enhances the mixing between the Higgs sector and the singlet sector. The leading contribution to λ_{eff} comes from the superpotential and D-terms.

Beyond these general results, we find a somewhat interesting feature because we focus on the parametric region analyzed by [3]. In this parametric region, an approximate \mathbb{S}_3 symmetry (permutation symmetry) arises due to the right handed neutrino generation independence of the non-Yukawa couplings and the smallness of the neutrino Yukawa couplings. Hence, to avoid any extra complications associated with domain wall formations, one might naively try to avoid \mathbb{S}_3 symmetry breaking phase transitions by considering parameters which yield zero temperature vacua preserving \mathbb{S}_3 . Hence, this is the boundary condition that we impose in this paper. Interestingly, we find that despite this boundary condition, \mathbb{S}_3 is typically spontaneously broken multiply at finite temperatures in a way that is sensitive to quantum radiative corrections. As the temperature is lowered from high temperatures, this leads to multi-step phase transitions starting from the trivially \mathbb{S}_3 symmetric vacuum in which all VEVs vanish. The electroweak symmetry breaking phase transition occurs with \mathbb{S}_3 symmetry *restoration* to a vacuum in which all sneutrino VEVs are identical and non-vanishing. We also find one step SFOPTs in which the scalar fields (including the singlet fields) make a transition from the origin to the electroweak symmetry breaking minimum. The numerical values of the parametric regions uncovered in this paper is in the paragraph containing Eq. (46) and regions IIIa and IIIb depicted in Fig. 5.

Since this work is most closely related to previous work on SFOPT in the NMSSM, we give here a little preview of some of the differences between our work and previous works, in addition to the multi-dimensional aspect stressed above. In Ref. [6], SFOPT in the context of the NMSSM is first analyzed and the author points out that the tree-level cubic term coming from the soft SUSY-breaking sector is important. Note that Ref. [6] uses the definition of critical temperature in which scalar mass squared matrix develops a vanishing eigenvalue. We take a more robust definition of T_c being the temperature at which a new coexistence phase occurs even though this definition is harder to implement in practice.

The authors of Ref. [7] also analyze the NMSSM, but they include a μ -term on the basis that it is more general and its nonzero value eliminates the \mathbb{Z}_3 symmetry which can be cosmologically dangerous with respect to the problem of domain wall formation [8]. The non-zero μ -term leads to false vacuum not being at the origin. In this case the critical temperature criterion used by Ref. [6] is invalid. Therefore, the authors of Ref. [7] take

the coexistence phase definition of critical temperature as we do in this paper. They also include a bilinear soft term in the Higgs which break the \mathbb{Z}_3 symmetry. Although we do not include such \mathbb{Z}_3 breaking terms directly, we will assume that non-renormalizable terms can be included to obtain acceptable phenomenology with respect to any possible domain wall formation. However, it is to be noted that \mathbb{Z}_3 breaking can often lead to UV instabilities in the singlet tadpoles, making the UV stability of these theories (including the one considered in this paper) a model building challenge as noted by [8].

The analysis [11] considers the generalized NMSSM similar to [7]. They run 9 parameters with a popular choice of “universal” boundary conditions from the GUT scale down to the electroweak scale to generate their model. They do not reject metastable vacua based on the intuition that longevity of the false vacuum on the horizon scale today is not difficult to attain. To be conservative and to avoid potentially complicated discussions of metastability, we accept only stable vacua in this paper.

A model related to the NMSSM and the $\mu\nu$ SSM is the nMSSM in which the discrete charge assignment is modified as to eliminate the singlet cubic term in the superpotential. This model was analyzed by [12] for SFOPT. For a significant portion of the parameter space in which SFOPT occurs, a linear tadpole term in the superpotential plays a significant role in contrast to our scenario.

The analysis of [13] considers the EWPT in an extension of the SM which adds a real singlet S . These authors find a large region of the parameter space of their model that is consistent with SFOPT and LEP Higgs search bounds. They argue that the strength of the phase transition can be enhanced by 1) choosing a large negative value for the SH^2 coupling, 2) choosing a negative value for the S^2H^2 coupling, or 3) allowing the singlet to have a non-zero VEV before the electroweak symmetry is broken. In the language of this paper, the first two points correspond to increasing E_{eff} and decreasing λ_{eff} , respectively.

Before we begin the main body of the work, let’s list here all the caveats to our analysis. We do not take into account explicitly the high energy Landau pole constraint (i.e. perturbativity up to the GUT scale) because we will take the attitude that the $\mu\nu$ SSM is well motivated mainly by its ability to have all fields participate at low energy and thereby have potential measurability. Nonetheless, the parametric region that we uncover lies at the border of perturbativity up to the GUT scale (inferring from the work of Refs. [3, 14]), which means that the UV cutoff for our theory can be taken to be far above the TeV scale. We do not take into account explicit \mathbb{Z}_3 breaking effects because small amount of breaking can address most cosmological domain wall problems, as we later demonstrate. We do not take into account explicit CP violation effects in the phase transitions as this will typically lead to less than order 10% effects since CP violating phases compatible with phenomenology are typically order 0.1 or smaller. For robustness, we accept in this paper as phenomenological possibility only absolutely stable global zero temperature vacua instead of analyzing the phenomenological possibilities of metastable vacua. Finally, all of our numerical work is kept in control to only order 10% accuracy.

The order of presentation is as follows. In the next section, we present the Lagrangian including its discrete symmetry properties and radiative/thermal corrections. The section concludes by highlighting the $\mu\nu$ SSM differences from the NMSSM scenario. In Sec. 3, we describe the parametric region relevant for SFOPT in terms of one-dimensional field space slice parameterization. There we also qualitatively describe how the multidimensional paths of the phase transition and discrete symmetries play a role. Next, in Sec. 4, we explicitly

show that singlets do not play a significant role in terms of numerical value of the sphaleron action controlling the $B + L$ violating rate in the broken phase. The main numerical results are presented in Sec. 5 where explicit existence of SFOPT parameter region is demonstrated. Details of the transition paths organized in terms of discrete symmetries, phenomenological bounds placed, and explicit mass spectra for a sample parametric point are given. In Sec. 6, we demonstrate that cosmological domain wall problem is easily evaded with an inclusion of a weak \mathbb{Z}_3 symmetry breaking operator in our scenario. We then conclude with a summary of the results. Several appendices then follow giving useful technical details. In Appendix A, we list the field dependent mass matrices used for computing the effective potential. In the next appendix, we give details regarding the approximate thermal masses used in the paper. In Appendix C, we describe analytically the boundaries of in Figure 5 which is one of our main results. Finally, in Appendix D, we show that it is generically possible to construct a non-renormalizable \mathbb{Z}_3 superpotential to obtain a CP conserving global minimum in the absence of any explicit CP violating parameters.

2. THE THERMAL POTENTIAL DIFFERENCES BETWEEN THE NMSSM AND THE $\mu\nu$ SSM

The $\mu\nu$ SSM that we consider in this paper is specified by the following superpotential and soft terms

$$W = \sum_i^3 \left\{ Y_u^i \hat{Q}_i \cdot \hat{H}_2 \hat{u}_i^c + Y_d^i \hat{H}_1 \cdot \hat{Q}_i \hat{d}_i^c + Y_e^i \hat{H}_1 \cdot \hat{L}_i \hat{e}_i^c + Y_\nu^i \hat{L}_i \cdot \hat{H}_2 \hat{\nu}_i^c - \lambda \hat{H}_1 \cdot \hat{H}_2 \hat{\nu}_i^c + \frac{1}{3} \kappa (\hat{\nu}_i^c)^3 \right\} \quad (3)$$

$$\begin{aligned} -\mathcal{L}_{\text{soft}} = & \sum_i^3 \left\{ m_{\tilde{Q}}^2 |\tilde{Q}_i|^2 + m_{\tilde{u}^c}^2 |\tilde{u}_i^c|^2 + m_{\tilde{d}^c}^2 |\tilde{d}_i^c|^2 + m_{\tilde{L}}^2 |\tilde{L}_i|^2 + m_{\tilde{e}^c}^2 |\tilde{e}_i^c|^2 + m_{\tilde{\nu}^c}^2 |\tilde{\nu}_i^c|^2 \right\} \\ & + \sum_i^2 m_{H_i}^2 |H_i|^2 - \frac{1}{2} \left(\sum_i^3 M_i \tilde{\lambda}_i \tilde{\lambda}_i + \text{h.c.} \right) + \sum_i^3 \left[-a_\lambda H_1 \cdot H_2 \tilde{\nu}_i^c + \frac{1}{3} a_\kappa (\tilde{\nu}_i^c)^3 + \text{h.c.} \right] \\ & + \sum_i^3 \left\{ a_u \tilde{Q}_i \cdot H_2 \tilde{u}_i^c + a_d H_1 \cdot \tilde{Q}_i \tilde{d}_i^c + a_e H_1 \cdot \tilde{L}_i \tilde{e}_i^c + a_\nu \tilde{L}_i \cdot H_2 \tilde{\nu}_i^c + \text{h.c.} \right\}. \quad (4) \end{aligned}$$

Where indicated by a dot, the $SU(2)$ indices are contracted with the antisymmetric tensor and $\epsilon_{12} = 1$. First, note in addition to the usual \mathbb{Z}_3 symmetry used to forbid an explicit μ term, there is an exact CP symmetry due to the reality of the coupling constants. We ignore the CKM phases since these will only give corrections smaller than the $\mathcal{O}(10\%)$ accuracy that we are aiming for in this paper. The CP transformation in the scalar effective potential effectively takes each scalar field to its complex conjugate. Next, note that the couplings of the $\tilde{\nu}_i^c$ sector to the SM were taken to be generation independent, except for the Yukawa couplings, and that the singlets do not couple to one another directly in the superpotential. This choice is motivated by trying partially to match the work of [3]. Hence, we see there is an enhanced \mathbb{S}_3 symmetry (permutation symmetry) in the $\tilde{\nu}_i^c$ sector if we neglect the Yukawa couplings. This approximate symmetry \mathbb{S}_3 is nearly exact because of the smallness of the symmetry breaking Yukawa couplings $Y_{e,\nu}^i$. As discussed in the introduction, the exact global

\mathbb{Z}_3 symmetry itself is plausibly assumed to be broken by non-renormalizable operators such that a cosmological domain wall problem does not arise.

At tree-level there is an additional global symmetry in the phase in which the electroweak symmetry is unbroken where $H_i = 0$ and all electromagnetically charged scalars vanish. Hence, in the high temperature phase in which the non-singlet fields are assumed to be frozen at their classical potential minimum, we have an enhanced symmetry in the effective potential as a function of the singlets only. The enhanced tree-level symmetry is $\mathbb{Z}_3 \otimes \mathbb{Z}_3 \otimes \mathbb{Z}_3$, where each singlet can be phase rotated independently:

$$\tilde{\nu}_j^c \longrightarrow e^{in_j 2\pi/3} \tilde{\nu}_j^c. \quad (5)$$

This symmetry appears because we have tuned the superpotential $\tilde{\nu}_1^c \tilde{\nu}_2^c \tilde{\nu}_3^c$ coupling to vanish. Unlike the approximate \mathbb{S}_3 symmetry, this high temperature phase classical symmetry has significant breaking at 1-loop from perturbative interactions even about the electroweak symmetry preserving minima. Nonetheless, this $(\mathbb{Z}_3)^3$ will be useful in understanding the SFOPT in which there is a rotation in the singlet sector space during the phase transition.¹

In addition to the Yukawa and gauge couplings, there are 19 adjustable parameters in this model which are $\{\lambda, \kappa, m_{\tilde{Q}, \tilde{u}^c, \tilde{d}^c, \tilde{L}, \tilde{e}^c, \tilde{\nu}^c}^2, m_{H_{1,2}}^2, M_i, a_{u,d,e,\nu,\lambda,\kappa}\}$. Because the neutrino Yukawa couplings control the neutrino Dirac mass via the up-type Higgs VEV, these Yukawas are small for reasonable values of $\tan \beta$,

$$Y_\nu \approx 6 \times 10^{-7} \left(\frac{\sin[\beta]}{\sin[\arctan 2.6]} \right)^{-1}, \quad (6)$$

and will play a negligible dynamical role. The neutral scalar components belonging to the fields $\{H_1, H_2, \tilde{L}_i, \tilde{\nu}_i^c\}$ have finite temperature VEVs denoted by

$$\langle H_i^0 \rangle_T = v_i(T), \quad \langle \tilde{\nu}_j^{(c)} \rangle_T = v_{\tilde{\nu}_j^{(c)}}(T) \quad j \in \{1, 2, 3\} \quad (7)$$

where the braces represent evaluating the field at the global minimum of the thermal effective potential Eq. (16). To maintain the \mathbb{S}_3 symmetry in the electroweak symmetry breaking vacuum at zero temperature and to avoid unnecessary complexities in the $SU(2)_L$ charged sector, we choose the sneutrino VEVs to be independent of generation, such that

$$\{v_i(0) = \text{real}, v_{\tilde{\nu}_i}(0) = v_{\tilde{\nu}}(0) = \text{real}, v_{\tilde{\nu}_i^c}(0) = v_{\tilde{\nu}^c}(0) = \text{real}\}. \quad (8)$$

To fix the VEVs in this way, we solve the potential minimization condition for the four parameters $\{m_{H_1}^2, m_{H_2}^2, m_L^2, m_{\tilde{\nu}^c}^2\}$. In addition to the desire to simplify the phase transition history, one of our main motivation in choosing $v_{\tilde{\nu}_i^c}(0) = v_{\tilde{\nu}^c}(0)$ is to preserve the \mathbb{S}_3 symmetry manifest in Eqs. (3) and (4). Interestingly enough, as we will see, this \mathbb{S}_3 symmetry spontaneously breaks at finite temperature. The left-handed sneutrino VEV is small, as we argue below,

¹ One may also wonder whether omitting the $\tilde{\nu}_1^c \tilde{\nu}_2^c \tilde{\nu}_3^c$ term is radiatively stable. It turns out that this term is generated at 2-loop order, which means that as far as one-loop analysis of this paper is concerned, this term can be omitted self-consistently. However, this must be viewed as fine tuning motivated by staying consistent with Ref. [3].

and the Higgs VEVs satisfy $v_1^2(0) + v_2^2(0) + 3v_{\tilde{\nu}}^2(0) \approx v_1^2(0) + v_2^2(0) = v^2(0) = (174 \text{ GeV})^2$. The rest of the parameter specification will be discussed in Sec. 5.

To study the electroweak phase transition we need to calculate the thermal effective potential V_{eff}^T as a function of temperature and the field directions which participate in the phase transition. There are no charged scalars with VEVs at zero temperature and we assume that there are no charge or color breaking minima to appear at finite temperature. In general, the left-handed sneutrinos receive VEVs $v_{\tilde{\nu}}(0)$ and participate in electroweak symmetry breaking, but these VEVs must be much less than the electroweak scale to avoid excessive stellar energy loss by $\tilde{\nu}$ emission [45]. Hence, we can neglect $\mathcal{O}(v_{\tilde{\nu}})$ contributions and reduce the relevant degrees of freedom to the five dimensional complex field space $\{H_1^0, H_2^0, \tilde{\nu}_i^c\}$. Although a part of the complex phase degrees of freedom in the Higgs sector is a gauge degree of freedom, for simplicity we will use the notation $\{H_1^0, H_2^0, \tilde{\nu}_i^c\}$ and keep in mind that there are nine real degrees of freedom.

We compute the zero temperature effective potential as a loop expansion over the field space $\{H_1^0, H_2^0, \tilde{\nu}_i^c\}$. The leading order term is the tree-level potential given by

$$\begin{aligned} V_0 = & m_{H_1}^2 |H_1^0|^2 + m_{H_2}^2 |H_2^0|^2 + m_{\tilde{\nu}^c}^2 \sum_i |\tilde{\nu}_i^c|^2 + \frac{g_1^2 + g_2^2}{8} \left(|H_1^0|^2 - |H_2^0|^2 \right)^2 \\ & + \sum_i \left[-a_\lambda H_1^0 H_2^0 \tilde{\nu}_i^c + \frac{1}{3} a_\kappa (\tilde{\nu}_i^c)^3 - \kappa \lambda (H_1^0 H_2^0)^* (\tilde{\nu}_i^c)^2 + \text{h.c.} \right] \\ & + 3\lambda^2 |H_1^0|^2 |H_2^0|^2 + |H_2^0|^2 \sum_i (Y_\nu^i)^2 |\tilde{\nu}_i^c|^2 + \lambda^2 \left(|H_1^0|^2 + |H_2^0|^2 \right) \left| \sum_i \tilde{\nu}_i^c \right|^2 + \kappa^2 \sum_i |\tilde{\nu}_i^c|^4. \end{aligned} \quad (9)$$

We exchange the three parameters $\{m_{H_1}^2, m_{H_2}^2, m_{\tilde{\nu}^c}^2\}$ for the real VEVs $\{v_1(0), v_2(0), v_{\tilde{\nu}^c}(0)\}$ by solving the three minimization equations

$$\begin{aligned} \left. \frac{\partial V_0}{\partial H_1^0} \right|_{\text{VEV}} = 0 &= m_{H_1}^2 v_1 + \frac{g_1^2 + g_2^2}{4} (v_1^2 - v_2^2) v_1 + 3 [-a_\lambda v_2 v_{\tilde{\nu}^c} - \kappa \lambda v_2 v_{\tilde{\nu}^c}^2] + 3\lambda^2 v_1 v_2^2 + 9\lambda^2 v_1 v_{\tilde{\nu}^c}^2 \\ \left. \frac{\partial V_0}{\partial H_2^0} \right|_{\text{VEV}} = 0 &= m_{H_2}^2 v_2 - \frac{g_1^2 + g_2^2}{4} (v_1^2 - v_2^2) v_2 + 3 [-a_\lambda v_1 v_{\tilde{\nu}^c} - \kappa \lambda v_1 v_{\tilde{\nu}^c}^2] + 3\lambda^2 v_2 v_1^2 + 9\lambda^2 v_2 v_{\tilde{\nu}^c}^2 \\ \left. \frac{\partial V_0}{\partial \tilde{\nu}_i^c} \right|_{\text{VEV}} = 0 &= m_{\tilde{\nu}^c}^2 v_{\tilde{\nu}^c} + [-a_\lambda v_1 v_2 + a_\kappa (v_{\tilde{\nu}^c}^2) - 2\kappa \lambda v_1 v_2 v_{\tilde{\nu}^c}] + 3\lambda^2 (v_1^2 + v_2^2) v_{\tilde{\nu}^c} + 2\kappa^2 v_{\tilde{\nu}^c} v_{\tilde{\nu}^c}^2 \end{aligned} \quad (10)$$

where ‘‘VEV’’ represents evaluating the fields at the zero temperature vacuum $\{H_1^0, H_2^0, \tilde{\nu}_i^c\} = \{v_1(0), v_2(0), v_{\tilde{\nu}^c}(0)\}$. Terms proportional to Y_ν^i and $v_{\tilde{\nu}}$ are negligible and have been omitted. Because of the \mathbb{S}_3 permutation symmetry of our potential, the three equations associated with the sneutrino field directions are identical.

The one-loop radiative correction to the effective potential is given by the Coleman-Weinberg potential [43] as a function of the field-dependent mass matrices M_i^2 calculated in the Landau gauge ($\xi = 0$). The mass matrices which we use are included in Appendix A along with n_i , the degrees of freedom associated with each matrix that correspond to suppressed indices (negative for fermions). Regulating UV divergences in $d = 4 - 2\epsilon$ dimensions, the

Coleman-Weinberg potential becomes

$$\Delta V_1^0 = \frac{1}{64\pi^2} \sum_i n_i \text{Tr} M_i^4 \left(\log \frac{M_i^2}{\mu^2} - \frac{3}{2} - C_{\text{UV}} \right) \quad (11)$$

where $C_{\text{UV}} = \frac{1}{\epsilon} - \gamma_E + \ln 4\pi$ and μ is the t'Hooft scale. We impose a mixed renormalization scheme in which the counterterms for the parameters $\{m_{H_1}^2, m_{H_2}^2, m_{\tilde{\nu}^c}^2\}$ are chosen such that the zero temperature vacuum is unshifted by the radiative corrections. This condition is equivalent to requiring tadpole graphs to vanish and imposes

$$\begin{aligned} \delta m_{H_1}^2 &= -\frac{1}{v_1} \left. \frac{\partial \Delta V_1^0}{\partial (H_1^0)^*} \right|_{\text{VEV}} \\ \delta m_{H_2}^2 &= -\frac{1}{v_2} \left. \frac{\partial \Delta V_1^0}{\partial (H_2^0)^*} \right|_{\text{VEV}} \\ \delta m_{\tilde{\nu}^c}^2 &= -\frac{1}{v_{\tilde{\nu}^c}} \left. \frac{\partial \Delta V_1^0}{\partial (\tilde{\nu}_i^c)^*} \right|_{\text{VEV}}. \end{aligned} \quad (12)$$

The remaining parameters are determined by the \overline{DR} scheme and all parameters are specified at a renormalization scale of $\mu = 100$ GeV. We make no assumptions about dominant contributions to the one-loop corrections but instead calculate Eq. (11) by summing all species that couple to the Higgs sector.

At finite temperature, the effective potential receives an additional one-loop correction

$$\Delta V_1^T = \frac{T^4}{2\pi^2} \left[\sum_b n_b \text{Tr} J_B (M_b^2/T^2) + \sum_f n_f \text{Tr} J_F (M_f^2/T^2) \right] \quad (13)$$

where the sums run over bosonic (b) and fermionic (f) mass matrices. The thermal functions can be expressed as a sum of modified Bessel functions of the second kind,

$$\begin{aligned} J_B(y) &= \int_0^\infty dx x^2 \log \left(1 - e^{-\sqrt{x^2+y}} \right) = - \sum_{n=1}^\infty \frac{1}{n^2} y K_2(n\sqrt{y}) \\ J_F(y) &= \int_0^\infty dx x^2 \log \left(1 + e^{-\sqrt{x^2+y}} \right) = - \sum_{n=1}^\infty \frac{(-1)^n}{n^2} y K_2(n\sqrt{y}). \end{aligned} \quad (14)$$

Because these integrals are computationally taxing, we use the Bessel function representation and truncate the sum at five terms. This is a very good approximation and introduces less than one percent of error.

At high temperatures, the perturbative expansion fails unless higher order ‘‘daisy’’ graphs which diverge quadratically with temperature are resummed. This procedure effectively replaces the bosonic field dependent mass matrix M_b^2 with $M_b^2 + \Pi_b$ where $\Pi_b \propto T^2$ and amounts to including a term into the potential given by

$$\Delta V_{\text{daisy}} = -\frac{T}{12\pi} \sum_b n_b \text{Tr} \left[(M_b^2 + \Pi_b)^{3/2} - (M_b^2)^{3/2} \right]. \quad (15)$$

The thermal mass corrections Π_b are included in Appendix B. Combining all of the radiative and finite temperature terms, the one-loop finite temperature effective potential plus daisy resummation is given by

$$V_{\text{eff}}^T(T) = V_0 + \Delta V_1^0 + \Delta V_1^T(T) + \Delta V_{\text{daisy}}(T). \quad (16)$$

The main difference between the NMSSM and the $\mu\nu$ SSM relevant for strongly first order EWPT can be summarized as follows:

1. Because of the multidimensionality of the singlet field space $\{v_{\tilde{\nu}_i^c}(T)\}$, there can be electroweak phase transitions accompanied by rotations within the singlet field space. This opens up a new class of phase transitions that are unlike any of the NMSSM transitions. For example, the phase transition can take place with the singlet VEV hopping from one nonzero value to another:

$$\{v_{\tilde{\nu}_i^c}(T_c) = x_i \neq 0, \langle H_j \rangle = 0\} \longrightarrow \{v_{\tilde{\nu}_i^c}(T_c) = y_i \not\parallel x_i, \langle H_j \rangle \neq 0\}. \quad (17)$$

The terms in Eqs. (3) and (4) that will play a particularly important role for this rotational hopping are the soft terms $-a_\lambda H_1 \cdot H_2 \tilde{\nu}_i^c + \frac{1}{3} a_\kappa (\tilde{\nu}_i^c)^3$ (which control the cubic and lower dimension tree-level couplings which in turn control radiative corrections) and the superpotential terms $-\lambda \hat{H}_1 \cdot \hat{H}_2 \hat{\nu}_i^c + \frac{1}{3} \kappa (\hat{\nu}_i^c)^3$ (which control the quartic and lower dimension tree-level couplings).²

2. There is a soft term coupling the singlet to the up-type Higgs,

$$\Delta V_{\text{soft}} \sim a_\nu \tilde{\nu}_i H_2^0 \tilde{\nu}_i^c, \quad (18)$$

which potentially provides a cubic coupling for the Higgs sector. Unfortunately, this term does not play an important role in the analysis because $v_{\tilde{\nu}} \ll \mathcal{O}(\text{GeV})$.

3. The superpotential has a Yukawa coupling of the singlet to the left-handed lepton and Higgs, leading to the following additional F -terms:

$$\begin{aligned} \Delta V_F = Y_\nu \sum_i \left[\kappa (H_2^0 \tilde{\nu}_i)^* (\tilde{\nu}_i^c)^2 - \lambda H_1^0 \left(|H_2^0|^2 \tilde{\nu}_i^* + \sum_j (\tilde{\nu}_j \tilde{\nu}_j^c)^* \tilde{\nu}_i^c \right) + \text{h.c.} \right] \\ + Y_\nu^2 \left(|H_2^0|^2 \sum_i (|\tilde{\nu}_i|^2 + |\tilde{\nu}_i^c|^2) + \left| \sum_i \tilde{\nu}_i \tilde{\nu}_i^c \right|^2 \right) \end{aligned} \quad (19)$$

Given the smallness of the Yukawa couplings $Y_\nu \sim \mathcal{O}(10^{-7})$, these terms are not particularly important for the phase transition when the transition occurs with VEVs of order 10^7 GeV or less. Note that all of these terms are quartic in nature owing to the absence of dimensionful parameters in the superpotential. Also, since the origin of R-parity violation is the leptonic Yukawa coupling which is also the source of ΔV_F , we see that these do not play a significant role.

Hence, a generic feature of the $\mu\nu$ SSM SF OPT not reproducible by the NMSSM is the feature due to point 1 above. This will be emphasized in the numerical exploration below. We will also find one step transitions, which are qualitatively similar to the NMSSM transitions.

² As we will see later, the shift of the field origin will generically generate lower dimension couplings from higher dimensional couplings.

3. QUALITATIVE DESCRIPTION OF THE DESIRED PARAMETRIC REGION

A novel feature of the $\mu\nu$ SJM compared to the NMSSM is the transition depicted in Eq. (17). In such cases one can shift the origin of the field such that the phase transition of interest occurs from the origin. With such shifted coordinates in mind, we define the field ϕ to be the radial magnitude

$$\phi \equiv \sqrt{(\vec{v})^2 + (\Delta\vec{v}_{\tilde{\nu}})^2 + (\Delta\vec{v}_{\tilde{\nu}c})^2} \quad (20)$$

for a phase transition controlled by the potential $V_T(\phi)$ in which the vector of CP-even Higgs scalars attains an order parameter change of \vec{v} . Explicitly, the strength of the phase transition is approximately characterized by the $SU(2)_L$ breaking $|\vec{v}|/T_c$ and not ϕ_c/T_c where the critical temperature T_c is defined by the condition $V_{T_c}(0) \approx V_{T_c}(\phi_c)$.

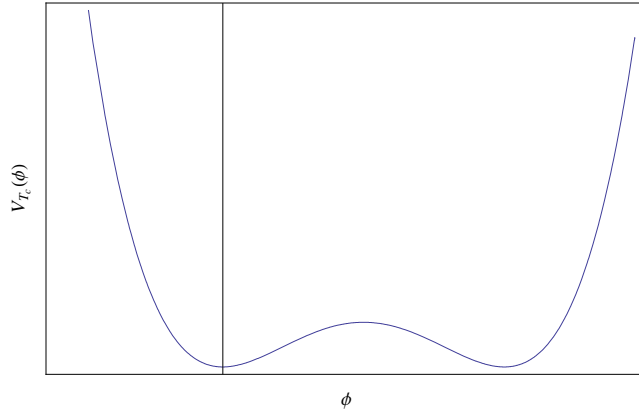


Figure 1: A schematic plot of the finite temperature effective potential at the critical temperature of Eq. (22). The vertical line represents $\phi = 0$ and helps to visualize the effect of $\phi \rightarrow -\phi$ symmetry breaking effect of the cubic term which is responsible for the bump at $\phi > 0$ for $\{E > 0, F_{\text{na}} = 0\}$ in Eq. (21).

The finite temperature corrected effective potential of a real scalar field ϕ near the critical temperature will behave approximately as

$$V_T(\phi) \approx \left(\frac{1}{2}M^2 + c_1T^2\right)\phi^2 - E_{\text{eff}}\phi^3 + F_{\text{na}}(\phi, T) + \frac{\lambda_{\text{eff}}}{4}\phi^4 + \text{other temperature dependences} \quad (21)$$

where $c_1 \sim \mathcal{O}(1)$ constant proportional to coupling constants responsible for the leading mass correction and F_{na} is the non-analytic thermal correction contribution that can lead to an effective cubic contribution to the potential. Although in the MSSM F_{na} plays a significant role, with a singlet involved such as in the $\mu\nu$ SJM, F_{na} need not play a crucial role. Hence, we will set $F_{\text{na}} = 0$. In this section, we neglect “other temperature dependences” in Eq. (21). Note that Eq. (21) has $M^2 > 0$ even though at $T = 0$, symmetry is broken when $E_{\text{eff}} > 0$ and satisfies a condition specified below.

Defining where $v(T_c)$ is the degenerate minimum VEV, we find

$$T_c = \frac{\sqrt{2E_{\text{eff}}^2/\lambda_{\text{eff}} - M^2}}{\sqrt{2c_1}}. \quad (22)$$

The potential at the critical temperature is depicted in Fig. 1. The unusual sign of $2E_{\text{eff}}^2/\lambda_{\text{eff}} - M^2$ stems from our assumption that the symmetry is broken at zero temperature due to predominantly the E_{eff} term. This situation turns out to be generically beneficial for a SFOPT as we explain soon below. The critical temperature T_c is larger if $E_{\text{eff}} > 0$ because in that case, the negative contribution from the cubic term in Eq. (21) is enhanced for $\phi > 0$ which means that the quadratic term which is the leading source of positivity (as ϕ approaches ϕ_c from the left) has to be stronger to cancel the stronger negative contribution. Since there will be no positive mass squared at the origin during the phase transition in the absence of the cubic term, the mass at the origin has to be also larger for increasing $E_{\text{eff}} > 0$. Explicitly, the mass at the origin (which by construction is our starting point of the phase transition) is

$$\partial_\phi^2 V_{T=T_c}(0) = \frac{2E_{\text{eff}}^2}{\lambda_{\text{eff}}}. \quad (23)$$

This mass is identical to the mass at $\phi = \phi_c$. We can also understand the VEV

$$\phi_c = \frac{2E_{\text{eff}}}{\lambda_{\text{eff}}} \quad (24)$$

which can be heuristically justified by the fact that the broken phase local minimum results from a competition between the cubic and the quartic term (which is the dominant source of positivity as $\phi \rightarrow \phi_c^+$) at the time of critical temperature when the mass term is again controlled by Eq. (23).

Finally, the strength of the $SU(2)_L$ breaking in the transition is given by

$$\frac{v(T_c)}{T_c} = \frac{v(T_c)\sqrt{2c_1}}{M\sqrt{\frac{2E_{\text{eff}}^2}{\lambda_{\text{eff}}M^2} - 1}} \quad (25)$$

where

$$v(T_c) = \phi_c f(\vec{\Omega}) \quad (26)$$

and $f(\vec{\Omega})$ is a projection cosine onto the Higgs axis. By definition of the $SU(2)_L$ breaking transition, $\phi_c f(\vec{\Omega}) \lesssim \mathcal{O}(v(0))$. At $T = 0$, $\phi(0) \equiv \langle \phi \rangle_{T=0}$ is related to M through

$$M = \sqrt{\lambda_{\text{eff}}\phi^2(0) - 3E_{\text{eff}}\phi(0)} \quad (27)$$

where $\lambda_{\text{eff}}\phi(0) > 3E_{\text{eff}}$. Eq. (25) thus can be rewritten in terms of $\phi(0)$ as

$$\frac{v(T_c)}{T_c} = \left(\frac{2E_{\text{eff}}}{\lambda_{\text{eff}}\phi(0)} \right) \frac{\sqrt{2c_1/\lambda_{\text{eff}}}}{\sqrt{\left(1 - \frac{E_{\text{eff}}}{\lambda_{\text{eff}}\phi(0)}\right) \left(1 - \frac{2E_{\text{eff}}}{\lambda_{\text{eff}}\phi(0)}\right)}} f(\vec{\Omega}). \quad (28)$$

Hence, the strength of the phase transition is controlled mostly by 2 parameters:

$$\left\{ \frac{E_{\text{eff}}}{\lambda_{\text{eff}}\phi(0)}, \sqrt{\frac{c_1}{\lambda_{\text{eff}}}} \right\}. \quad (29)$$

Note that since $f(\vec{\Omega}) \leq 1$, this angular projection function can only enhance the phase transition in a limited manner. Requiring $\frac{v(T_c)}{T_c}$ be real and $V(\phi(0)) < V(0)$ result in the condition

$$0 \leq \frac{E_{\text{eff}}}{\lambda_{\text{eff}}\phi(0)} \leq \frac{1}{2}. \quad (30)$$

Therefore, one should keep in mind that although having a non-vanishing E_{eff} is good for a strong first order phase transition, the enhancement is bounded. Indeed, this bound is approximately satisfied by the numerical analysis, and SFOPT points that we find occur when

$$\frac{E_{\text{eff}}}{\lambda_{\text{eff}}\phi(0)} \approx \frac{1}{2}. \quad (31)$$

From the derivation of Eq. (28), one can see that Eq. (31) corresponds to making T_c as small as possible during the phase transition. When $\frac{E_{\text{eff}}}{\lambda_{\text{eff}}\phi(0)} > \frac{1}{2}$ the origin becomes the global minimum and the symmetry is unbroken. Note also that because ϕ is defined with respect to the shifted singlet origin in Eq. (20), $\phi(0)$ does not correspond to the radial magnitude of the scalar field from the original Lagrangian's field origin.

After this first order phase transition, a second order phase transition might occur when $V''(0) = 0$. However, with $M^2 > 0$, this does not occur for this 1D toy model. Note that [6] assumes that there exists a temperature for which $V'' = 0$ which in fact never occurs for this toy model.

Generically, we are interested in a strong first order phase transition characterized by

$$\sqrt{2}\frac{v(T_c)}{T_c} \gtrsim 1.3 \quad (32)$$

[5]. If the asymptotic conditions $\frac{E_{\text{eff}}}{\lambda_{\text{eff}}\phi(0)} \rightarrow 1/2$ and/or $c_1/\lambda_{\text{eff}} \rightarrow \infty$ are met, the phase transition can be arbitrarily strong. However, the following phenomenological constraints prevent/constrain an arbitrarily strong transition in Eq. (28):

1. Global minima shifts can prevent the saturation of $E_{\text{eff}}/[\lambda_{\text{eff}}\phi(0)] = 1/2$ for a particular underlying parametric path. For example, as one approaches $E_{\text{eff}}/[\lambda_{\text{eff}}\phi(0)] = 1/2$ within a particular region of underlying parameter space,³ the origin of Eq. (20) has to be shifted to a new global minimum (where the electroweak symmetry is still not broken, i.e. $\vec{v} = 0$). When this occurs, $\{E_{\text{eff}}, \lambda_{\text{eff}}, c_1\}$ of Eq. (21) undergo a discontinuous change as a function of the underlying parameters such as those of Eqs. (3) and (4).
2. Small λ_{eff} can result in phenomenologically unacceptably light Higgs (or other scalar masses). For example, it is clear from the effective model that

$$m_\phi^2 = 2\lambda_{\text{eff}}\phi^2(0) \left[1 - \frac{3}{2} \frac{E_{\text{eff}}}{\lambda_{\text{eff}}\phi(0)} \right] \quad (33)$$

³ Recall that $E_{\text{eff}}/[\lambda_{\text{eff}}\phi(0)]$ are effective parameters derivable from underlying Lagrangian parameterized for example as Eqs. (3) and (4).

where the term in the parenthesis in Eq. (33) is positive since $0 \leq E_{\text{eff}}/(\lambda_{\text{eff}}\phi(0)) \leq 1/2$. Note that in any models that embed the MSSM, there is a minimal contribution to λ_{eff} from the D-terms that also makes it difficult to make it arbitrarily small. Note also that increasing $\frac{E_{\text{eff}}}{\lambda_{\text{eff}}\phi(0)}$ lowers the ϕ mass as well.

3. When $E_{\text{eff}}/(\lambda_{\text{eff}}\phi(0)) \rightarrow 1/2$, the energy difference ΔV between the false vacuum and true vacuum asymptotically vanishes. Explicitly, we have as $E_{\text{eff}} \rightarrow E_c \equiv \lambda_{\text{eff}}\phi(0)/2$, we find

$$\Delta V \rightarrow \frac{2\sqrt{2}\Delta E_{\text{eff}}M^3}{\lambda^{3/2}} \rightarrow 0 \quad (34)$$

$$\frac{v(T_c)}{T_c} \rightarrow \left(\frac{2}{\lambda_{\text{eff}}}\right)^{1/4} \sqrt{\frac{c_1 M}{\Delta E_{\text{eff}}}} \quad (35)$$

where $\Delta E_{\text{eff}} \equiv E_{\text{eff}} - E_c$. Since the validity of this estimate requires $\Delta V > 0$, this region of parameter space becomes very sensitive to radiative corrections.

4. The contributions to c_1 that maximize $\sqrt{c_1/\lambda_{\text{eff}}}$ typically contribute to λ_{eff} as well (with different powers). Hence, particularly in the $\mu\nu$ S SM, we are in a region where λ_{eff} is on the larger side and not the small side.

The features just discussed qualitatively explain the numerical scan of the parameter space which identifies a particular parametric region in which Eq. (32) is satisfied at the same time with some basic phenomenological constraints which we detail in Sec. 5. There, more analytic formulae will be given explaining some of the features of the numerical results.

Now, let us consider the general path of the electroweak phase transition. At $T \gg \mathcal{O}(\text{TeV})$, the global minimum will be at

$$\{v_{\tilde{\nu}_i^c}(T) = 0, v_i(T) = 0\}, \quad (36)$$

the scalar field origin.⁴ As explained previously, the left-handed slepton VEVs are undergoing small energy scale transitions which are not particularly relevant to most of the discussion. As the temperature is lowered, a non-trivial singlet VEV configuration will realize a global minimum, and the system will consequently make a transition. This transition in the singlets is sometime accompanied by an electroweak symmetry breaking phase transition and sometimes not. If the first nontrivial singlet transition is accompanied by strongly first order electroweak symmetry breaking, these would be SFOPT from the scalar field origin:

$$\{v_{\tilde{\nu}_i^c}(T_c^+) = 0, v_j(T_c^+) = 0\} \longrightarrow \{v_{\tilde{\nu}_i^c}(T_c^-) \neq 0, v_j(T_c^-) \neq 0\}. \quad (37)$$

In this case, the origin of the vector whose magnitude is taken in Eq. (20) will be zero.

In addition, there will generically be singlet transitions from the origin at temperature T_O first without an electroweak phase transition, of the form

$$\{v_{\tilde{\nu}_i^c}(T_O^+) = 0, v_j(T_O^+) = 0\} \longrightarrow \{v_{\tilde{\nu}_i^c}(T_O^-) = x_i(T_O) \neq 0, v_j(T_O^-) = 0\}. \quad (38)$$

⁴ Symmetry restoration typically occurs as long as there are no tadpole contribution proportional to the temperature.

Even if this is a first order phase transition, it will typically complete before the subsequent electroweak symmetry breaking, and thus it does not, to leading approximation, participate in EWBG. However, it can in principle be relevant for gravity waves (see e.g. [15–42]). Afterwards, there is a subsequent electroweak symmetry breaking phase transition

$$\{v_{\tilde{\nu}_i^c}(T_c^+) = x_i(T_c) \neq 0, v_j(T_c^+) = 0\} \longrightarrow \{v_{\tilde{\nu}_i^c}(T_c^-) = y_i \neq 0, v_j(T_c^-) \neq 0\} \quad (39)$$

whose strength is important for EWBG. In this case, the origin of the vector whose magnitude is taken in Eq. (20) will be $\{v_{\tilde{\nu}_i^c}(T_c^+) = x_i, v_j(T_c^+) = 0\}$. When $x_i \not\parallel y_i$, this transition corresponds to a “rotation” of the singlet vector.

Before concluding this section, let’s briefly describe how the discrete symmetry discussed below Eq. (4) and zero temperature radiative corrections play a role for some of our strong multi-step transitions. Once a phase transition of the form Eq. (38) takes place, the set of degenerate global minima will form a coset representation of $\mathbb{Z}_3 \otimes \text{CP} \otimes \mathbb{S}_3$.⁵ Because of the approximate $\mathbb{Z}_3 \otimes \mathbb{Z}_3 \otimes \mathbb{Z}_3$ symmetry described in Eq. (5), to tree-level accuracy, the coset space will be actually bigger: $\mathbb{Z}_3 \otimes \mathbb{Z}_3 \otimes \mathbb{Z}_3 \otimes \text{CP} \otimes \mathbb{S}_3$. Some of the $\mathbb{Z}_3 \otimes \mathbb{Z}_3 \otimes \mathbb{Z}_3$ minima will be split due to the zero temperature radiative corrections, and the global minimum will be at a subset of the $\mathbb{Z}_3 \otimes \mathbb{Z}_3 \otimes \mathbb{Z}_3$ minima (one of which is what we labeled as $\vec{x}(T_O)$ in Eq. (38)). Finally, when the temperature drops enough to make one of the EWSB minima degenerate with $\vec{x}(T_c)$, the transition depicted by Eq. (39) occurs.

In Sec. 5, we will discuss explicit examples of both one step and multi-step phase transitions.

4. WEAK SPHALERON AND THE SINGLET

After the baryon asymmetry has been created at a first order electroweak phase transition, it may be washed out by the B-violating sphaleron process [4, 46] in the broken phase. The sphaleron is a non-perturbative field configuration in the Weinberg-Salam theory that interpolates between topologically distinct vacua and violates $B + L$. To avoid washout, one must require that sphaleron transitions are suppressed meaning that the rate of these processes is less than the Hubble parameter at the time of the phase transition. This imposes a lower bound on the sphaleron Euclidean action $E_{\text{sph}}(T_c)/T_c \gtrsim 45$ [5] which, in the Standard Model, becomes a lower bound on the Higgs VEV in the broken phase $\sqrt{2}v(T_c)/T_c \gtrsim 1.3$ where $v(0) = 174$ GeV. The six sneutrino fields of the $\mu\nu\text{SSM}$ which receive VEVs during EWSB could in principle modify this bound. As we will see, the modifications are small because 1) the left-handed sneutrino VEV is much less than the electroweak scale and 2) the singlet sneutrino has a nearly homogenous solution which stays nears the minimum of the potential.

To obtain the sphaleron action at finite temperature, we calculate the zero temperature sphaleron and apply the scaling law [47]

$$E_{\text{sph}}(T) = E_{\text{sph}}(0) \frac{v(T)}{v(0)} \quad (40)$$

⁵ Recall that \mathbb{S}_3 is nearly an exact symmetry because of the smallness of the leptonic Yukawa coupling.

which introduces less than a ten percent error. Additionally, we compute the sphaleron solution using the tree-level scalar potential V_0 and neglect radiative corrections. To a very good approximation [46] we can also neglect the $U(1)_Y$ gauge coupling and compute a purely $SU(2)_L$ sphaleron solution. The sphaleron ansatz is static and possesses an $SO(3)$ rotational symmetry. The ansatz is given by

$$\begin{aligned} \{H_1, H_2, \tilde{L}_i\} &= \{v_1 h_1(\xi), v_2 h_2(\xi), v_3 h_3(\xi)\} U^\infty \begin{pmatrix} 0 \\ 1 \end{pmatrix} \\ \tilde{\nu}_i^c &= v_4 h_4(\xi) \\ W_i^a \sigma^a dx^i &= -\frac{2i}{g} f(\xi) dU^\infty (U^\infty)^{-1} \end{aligned} \quad (41)$$

$$U^\infty = \frac{1}{r} \begin{pmatrix} z & x + iy \\ -x + iy & z \end{pmatrix} \quad (42)$$

in terms of the dimensionless radial coordinate $\xi = r/r_0$ rescaled by $r_0 = (g\sqrt{2}\sqrt{v_1^2 + v_2^2 + v_{\tilde{\nu}}^2})^{-1} \approx (g\sqrt{2}v)^{-1}$. All VEVs are evaluated at zero temperature and we have introduced $v_3 = v_{\tilde{\nu}}$ and $v_4 = v_{\tilde{\nu}^c}$ for convenience. We have used the \mathbb{S}_3 symmetry to equate the functions that describe the sneutrino fields of different generations, such that the sphaleron solution is given by five functions $h_i(\xi)$ and $f(\xi)$. With this ansatz the field equations become

$$\begin{aligned} \frac{\xi^2 r_0^2}{v_i^2} \frac{\partial V_0}{\partial h_i} &= \begin{cases} \xi^2 h_i'' + 2\xi h_i' - 2(1-f)^2 h_i & i = 1, 2 \\ 3[\xi^2 h_3'' + 2\xi h_3' - 2(1-f)^2 h_3] & i = 3 \\ 3[\xi^2 h_4'' + 2\xi h_4'] & i = 4 \end{cases} \\ \xi^2 f'' - 2f(1-f)(1-2f) &= -\frac{1}{4} \xi^2 (1-f) (v_1^2 h_1^2 + v_2^2 h_2^2 + 3v_3^2 h_3^2) g^2 r_0^2. \end{aligned} \quad (43)$$

where the potential is normalized to vanish in the EWSB vacuum $V_0(h_i = 1) = 0$. Note that the term $(1-f)^2 h_i$ is absent for $i = 4$ because the singlet sneutrinos do not couple to the gauge bosons. The sphaleron action is obtained by integrating the sphaleron solution

$$\begin{aligned} E_{\text{sph}}(0) &= \frac{4\pi v\sqrt{2}}{g} \int_0^\infty \left\{ 4 \left(\frac{df}{d\xi} \right)^2 + \frac{8}{\xi^2} f^2 (1-f)^2 + \xi^2 \frac{V_0(h_i)}{g^2 v^4} \right. \\ &\quad \left. + \frac{\xi^2}{2v^2} \left[\left(v_1 \frac{dh_1}{d\xi} \right)^2 + \left(v_2 \frac{dh_2}{d\xi} \right)^2 + 3 \left(v_3 \frac{dh_3}{d\xi} \right)^2 + 3 \left(v_4 \frac{dh_4}{d\xi} \right)^2 \right] \right. \\ &\quad \left. + \frac{1}{v^2} (v_1^2 h_1^2 + v_2^2 h_2^2 + 3v_3^2 h_3^2) (1-f)^2 \right\} d\xi \end{aligned} \quad (44)$$

We can observe immediately that contributions from the left-handed sneutrinos will be negligible because the function h_3 always appears with a prefactor of $v_3 = v_{\tilde{\nu}} \ll v$.

We can study the sphaleron solution by considering the asymptotic limits of Eq. (43). In the large ξ limit, all five field profiles must asymptote to unity in order for E_{sph} to be finite. In the small ξ limit, we find that the gauge boson and the three weakly charged scalar

functions asymptote to zero, as in the Weinberg-Salam model, but that the singlet function approaches a value which can in general be non-zero:

$$f(\xi) \xrightarrow{\xi \rightarrow 0} \alpha \xi^2, \quad h_i(\xi) \xrightarrow{\xi \rightarrow 0} \beta_i \xi \quad i \in \{1, 2, 3\}, \quad h_4 \xrightarrow{\xi \rightarrow 0} c + \beta_4 \xi^2. \quad (45)$$

The singlet function behaves differently in this limit because the gauge coupling term $(1 - f)^2 h_4$ in the field equation is absent. The boundary condition on the singlets makes the solution for $h_4(\xi)$ qualitatively different than for the Higgs fields. In particular, the solution $h_4(\xi)$ which minimizes E_{sph} will tend to be homogenous with $h_4 \approx 1$ for all ξ . The solution is homogenous because $E_{\text{sph}} \ni (dh_4/d\xi)^2$ is positive semi-definite. Hence, it can be minimized by a constant h_4 , and the solution remains near $h_4 = 1$ because this is where V_0 is minimized. As a result, the singlet fields contribute negligibly to the sphaleron action.

The sphaleron solution and energy density for a fiducial parameter set are plotted in Figure 2. To obtain the field profiles we solve Eq. (43) in the large and small ξ limits analytically, then match the solutions at five radii r_i which are chosen to minimize E_{sph} . As discussed above, the singlet solution hovers around $h_4 = 1$ where the potential has a minimum. To display how each terms in Eq. (44) contributes to the sphaleron action, we have also plotted the integrand for the gauge kinetic, scalar kinetic, and scalar potential contributions separately. We observe that the sphaleron action is dominated by the kinetic terms. Since the parametric dependence only appears explicitly in the scalar potential, which is negligible, we expect that the sphaleron action is largely independent of our parameter choice. For this parameter set we find $E_{\text{sph}}(0) \approx 1.83 \frac{4\pi v}{g} \approx 8.7$ TeV which translates into a bound on the Higgs VEV at the critical temperature that is $\sqrt{2} \frac{v(T_c)}{T_c} \gtrsim 1.3$. As such, the Higgs VEV must satisfy the same constraint in the $\mu\nu$ SSM as in the SM to avoid washout.

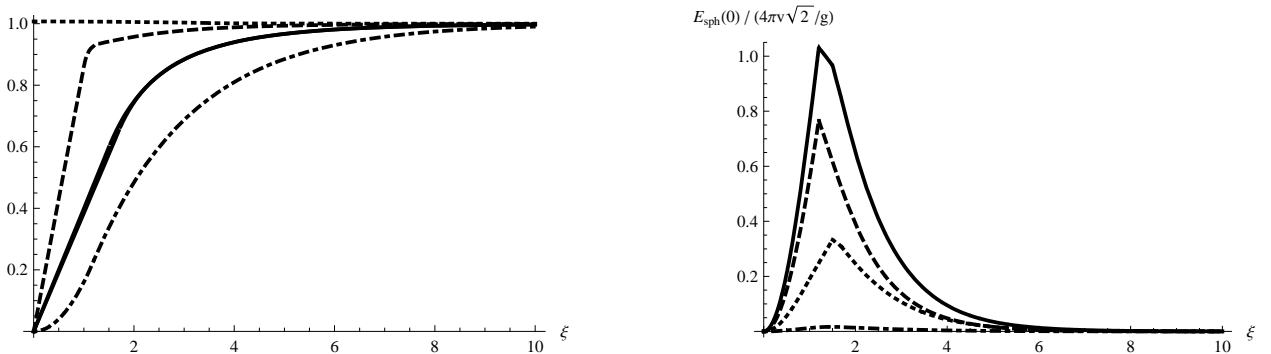


Figure 2: On the left, the $\mu\nu$ SSM sphaleron solution versus the dimensionless radial coordinate with h_1 and h_2 solid, h_3 dashed, h_4 dotted, and f dot-dashed. The solution $h_{\tilde{\nu}c}$ for the singlet sneutrinos does not satisfy the same boundary condition at $\xi \rightarrow 0$ as the $SU(2)_L$ charged scalars. Hence, the solution of minimum energy is the one in which $h_{\tilde{\nu}c} \approx 1$ for all ξ . On the right, the sphaleron energy density, Eq. (44), with gauge kinetic terms dashed, scalar kinetic terms dotted, scalar potential terms dot-dashed, and the total energy density solid. This plot illustrates that the sphaleron action is dominated by the kinetic terms and that the contribution from the scalar potential is negligible.

5. PARAMETER SCAN AND PHENOMENOLOGICAL BOUNDS

We have investigated the $\mu\nu$ SSM phase transition by performing a two-dimensional parameter space scan. For the two free parameters we use $m_{\text{ch}} = 3\lambda v_{\bar{\nu}^c}$, which coincides with the charged Higgsino mass in the limit $M_2 \gg m_W, m_{\text{ch}}$, and the dimensionless variable

$$\sigma = 2 \left(\frac{a_\lambda}{m_{\text{ch}}\lambda} + \frac{\kappa}{3\lambda} \right). \quad (46)$$

These parameters are scanned uniformly over the ranges $m_{\text{ch}} : [75 \text{ GeV}, 175 \text{ GeV}]$ and $\sigma : [0, 25]$ by varying $v_{\bar{\nu}^c}$ and a_λ . The SUSY-breaking parameters are chosen to match the conventions of [3]: $\{m_{\tilde{Q}}^2, m_{\tilde{u}^c}^2, m_{\tilde{d}^c}^2, m_{\tilde{e}^c}^2\}$ are fixed at a fiducial SUSY-breaking scale which is taken to be 1 TeV, gaugino masses are set to $6M_1 = 3M_2 = M_3 = 3 \text{ TeV}$, and A-terms are scaled by the associated Yukawa couplings as $\{A_{u_i} = a_{u_i}/Y_{u_i}, A_{d_i} = a_{d_i}/Y_{d_i}, A_{e_i} = a_{e_i}/Y_{e_i}, A_\nu = -a_\nu/Y_\nu\}$ and fixed at 1 TeV. Note that we have assumed for simplicity common left-handed sneutrino VEVs $v_{\tilde{\nu}_i} = v_{\tilde{\nu}}$ and a diagonal Yukawa matrix $(Y_\nu)_{ij} = Y_\nu \delta_{ij}$. The remaining soft masses $\{m_{H_1}^2, m_{H_2}^2, m_L^2, m_{\bar{\nu}^c}^2\}$ are exchanged for the VEVs $\{v_1(0), v_2(0), v_{\tilde{\nu}}(0), v_{\bar{\nu}^c}(0)\}$ by solving the minimization equations at zero temperature. The remaining Higgs sector parameters are chosen to be $\tan\beta = 2.6, \kappa = -0.64, \lambda = 0.18, v_{\tilde{\nu}} = 1.4 \times 10^{-5} \text{ GeV}$, and $a_\kappa = -236 \text{ GeV}$. Given that some of our sparticle masses are far larger than $T_c \sim \mathcal{O}(100)\text{GeV}$, we could have integrated out these fields giving rise to a more illuminating effective field theory parameterization within the \overline{DR} scheme.⁶ However, to stay similar to the parameterization used in [2, 3], and to give a relatively unrestricted range for possible T_c , we have kept these relatively heavy fields as dynamical.

At each point in the parameter space, we calculate the $\mu\nu$ SSM spectrum. In order to get a handle on phenomenological constraints, we impose the MSSM search bounds for the SUSY particles and require the Higgs masses to be $\gtrsim 90 \text{ GeV}$ [48] (later we will show a sample parametric point Higgs spectrum with the lightest Higgs mass of about 110 GeV). Model dependent bounds are of interest, but typically they are weaker, as far as the neutral Higgs is concerned, because of singlet mixing effects. A more complete model dependent phenomenological consistency check including the study of charged Higgs mediated $b \rightarrow s\gamma$ rates is beyond the scope of this paper. We calculate the spectrum of the charged Higgses (ϕ_i^\pm), charginos ($\tilde{\chi}_i^\pm$), and neutralinos ($\tilde{\chi}_i^0$) at tree-level and require $\{m_{\phi_1^\pm} > 79.3 \text{ GeV}, m_{\tilde{\chi}_1^\pm} > 94 \text{ GeV}, m_{\tilde{\chi}_1^0} > 46 \text{ GeV}\}$. The SM-like neutrinos mix with the neutralinos and heavy neutrinos in a seesaw matrix. We are able to reproduce the correct neutrino mass scale but neglected the question of precise neutrino mass pattern since any desired neutrino mass pattern will not be difficult to achieve by adjusting the small Yukawa couplings. Since we have already noted that the smallness of the leptonic Yukawa couplings make their role in the current SFOT analysis insignificant, this does not present a significant loss of generality.

Because the squark, charged slepton, and left-handed sneutrino masses are supported by their TeV-scale SUSY-breaking mass parameters, they are insensitive to parameters in

⁶ Recall that in \overline{DR} scheme, decoupling is accomplished “by hand” through computing threshold corrections after integrating out fields.

the Higgs sector and are not affected by the phenomenological lower bounds. We compute the mass spectrum of Higgses and singlet sneutrinos at one-loop order using the effective potential. Since we choose the VEVs for these fields to be real and there is no explicit CP-violation, the CP-even (ϕ_i) and CP-odd (a_i) components do not mix. The mass matrices are given by the curvature of the one-loop effective potential evaluated at the zero temperature vacuum ⁷

$$(M_\phi^2)_{ij} = \frac{\partial^2 V_{\text{eff}}^0}{\partial(\mathcal{R}\varphi_i)\partial(\mathcal{R}\varphi_j)} \Big|_{\text{VEV}} \quad (M_a^2)_{ij} = \frac{\partial^2 V_{\text{eff}}^0}{\partial(\mathcal{I}\varphi_i)\partial(\mathcal{I}\varphi_j)} \Big|_{\text{VEV}} \quad (47)$$

where $\varphi_i \in \{H_1^0, H_2^0, \tilde{\nu}_j^c\}$. We can separately impose the mass bounds $m_{\phi_1} > 92.8$ GeV and $m_{a_1} > 93.4$ GeV.

At each point in parameter space that satisfies the phenomenological mass bounds, we require the electroweak-breaking vacuum with $v(0) = 174$ GeV to be the global minimum of the one-loop effective potential. This condition imposes particularly strong constraints on the parameter space. To understand these constraints and the nature of our multi-step phase transitions, we must discuss the structure of the $\{H_1^0, H_2^0, \tilde{\nu}_i^c\}$ field space and, in particular, determine the locations of the vacua that could potentially have lower energy than the EWSB vacuum. Recall that in the subspace with $H_1^0 = H_2^0 = 0$ there is a $\mathbb{Z}_3 \otimes \mathbb{Z}_3 \otimes \mathbb{Z}_3$ symmetry at tree-level given by Eq. (5). To locate the extrema in this field space we solve the three cubic equations

$$\frac{\partial V_0}{\partial \tilde{\nu}_i^c} \Big|_{H_1^0=H_2^0=0} = 0 \quad i \in \{1, 2, 3\} \quad (48)$$

for $\tilde{\nu}_i^c$. The solutions of Eq. (48) which turn out to be minima (for our choice of the sign of a_κ) are given by

$$\begin{aligned} \tilde{\nu}_i^c &= \rho_i e^{in_i \frac{2\pi}{3}} & n_i &\in \{0, 1, 2\} \\ \rho_i &= 0 \quad \text{or} \quad \frac{1}{4\kappa^2} \left(-a_\kappa + \sqrt{a_\kappa^2 - 8m_{\tilde{\nu}^c}^2 \kappa^2} \right) && \approx v_{\tilde{\nu}^c} \end{aligned} \quad (49)$$

We will focus on the solutions with $\rho_1 = \rho_2 = \rho_3 \approx v_{\tilde{\nu}^c}$ because these minima are in general deeper than those with $\rho_i = 0$. Then, there are $3^3 = 27$ local minima in the $H_1^0 = H_2^0 = 0$ field space, that we will refer to by $\vec{x}_{n_1 n_2 n_3}$ where the subscript indicates the phases of the three singlets. The $(\mathbb{Z}_3)^3 \otimes \mathbb{S}_3 \otimes \text{CP}$ symmetry ensures the degeneracy of the twenty-seven minima. Moving away from $H_1^0 = H_2^0 = 0$ as illustrated in Figure 3, the $(\mathbb{Z}_3)^3$ symmetry is broken to \mathbb{Z}_3 by terms in V_0 proportional to a_λ and λ . We will use $\vec{y}_{n_1 n_2 n_3}$ to denote the point in field space near to $\vec{x}_{n_1 n_2 n_3}$ but where $H_1^0/v_1 = H_2^0/v_2 = 1$. For example, in this notation, \vec{y}_{000} corresponds to the EWSB vacuum in which the three singlets have real VEVs.

At one-loop order, radiative corrections break the approximate $(\mathbb{Z}_3)^3$ symmetry (described above Eq. (5)) and split the degeneracy of the $\vec{x}_{n_1 n_2 n_3}$ minima as represented by Figure 4.

⁷ Since the effective potential is defined as a sum over 1PI diagrams with zero external momentum, this definition of mass differs from the pole in the propagator by the difference of the scalar self-energy evaluated at $p = m_{\text{pole}}$ and $p = 0$.

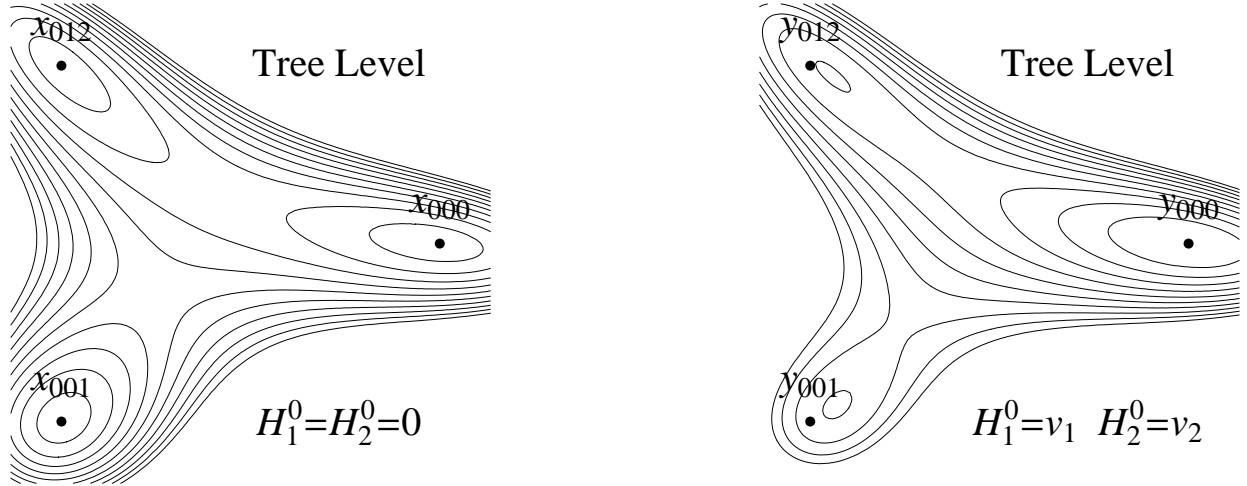


Figure 3: The tree-level potential plotted over a slice of the $\tilde{\nu}_i^c$ field space with $H_1^0 = H_2^0 = 0$ on the left and $H_1^0/v_1 = H_2^0/v_2 = 1$ on the right. The labeled points are defined in the text, and a stationary point of the potential can be found at or near each of the labeled points. The potential grows farther from the central region. In the EW-preserving subspace, the three minima are degenerate, but the Higgs VEV selects out \vec{y}_{000} as the global minimum.

After including radiative corrections, the preserved symmetry group is $\mathbb{Z}_3 \otimes \mathbb{S}_3 \otimes \text{CP}$. (Here, as an approximation, we are ignoring the fact that the subgroup $\mathbb{S}_3 \otimes \text{CP}$ is explicitly weakly broken in the Lagrangian already while \mathbb{Z}_3 must be broken by non-renormalizable operators to evade cosmological inconsistencies caused by domain walls.) The 27-fold degeneracy is split into three classes: a 3-fold degeneracy of the points \vec{x}_{iii} , a 6-fold degeneracy of the points \vec{x}_{ijk} for $i \neq j \neq k$, and a 18-fold degeneracy of the points \vec{x}_{ijj} plus permutations for $i \neq j$. In order to discuss the phase transition we will choose one representative from each class: \vec{x}_{000} , \vec{x}_{012} , and \vec{x}_{001} . In this notation, if we say a transition occurs from the origin to \vec{x}_{012} we mean that just below the critical temperature the vacuum is localized nearby to one of the six field points in the class that contains \vec{x}_{012} .

The radiative corrections will generally split the degeneracy in such a way that some of the EW-preserving vacua will be depressed relative to the EWSB vacuum and may cause the latter to become metastable. This is both good and bad for the parameter space scan and phase transition analysis. It is bad because many points will be excluded because the EWSB vacuum is only metastable. On the other hand, it is good because with appropriate tuning, we can obtain an EW-preserving vacuum that is nearly degenerate with, but slightly higher than, the EWSB vacuum. Along the trajectory connecting these vacua, we can make $E_{\text{eff}}/(\lambda_{\text{eff}}\phi(0))$ arbitrarily close to one half and obtain SFOPT. In Appendix C we include analytic bounds which must be satisfied to prevent the EWSB vacuum from becoming metastable.

At each point in parameter space which satisfies the mass and vacuum bounds described above, we calculate the critical temperature, T_c , and Higgs VEV, $v(T_c)$, at the electroweak phase transition. The phase transition is calculated using the following procedure: increase the temperature from zero in increments, at each temperature minimize the thermal effective

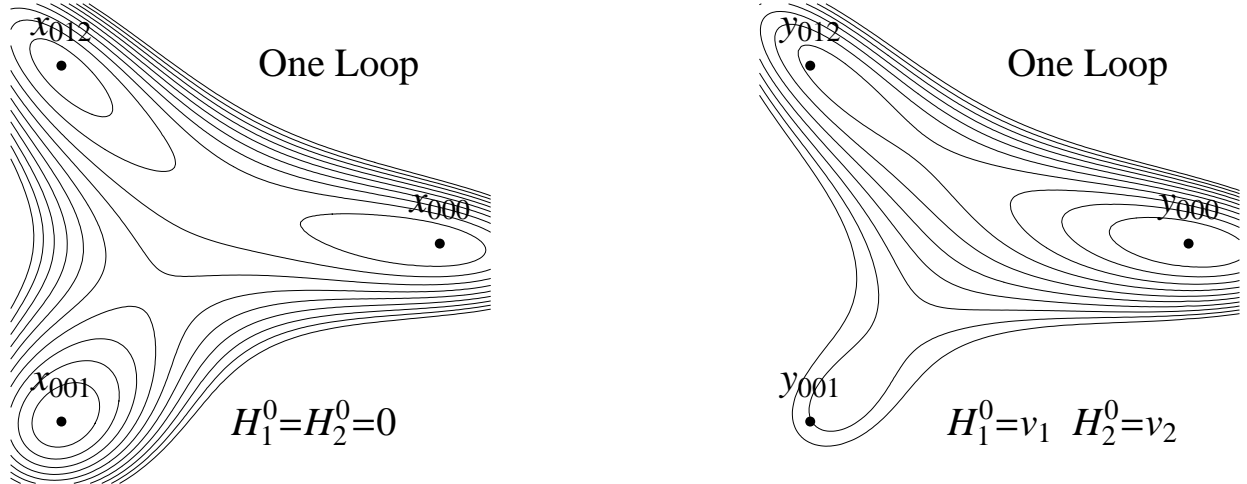


Figure 4: Same as Figure 3 but the contours represent values of the one-loop effective potential at zero temperature. The degeneracy is broken even in the EW-preserving subspace and induces $V_1^0(\vec{x}_{012}) < V_1^0(\vec{x}_{001}) < V_1^0(\vec{x}_{000})$.

potential to find the EWSB vacuum $\vec{v}_{EWSB}(T) = \{v_1(T), v_2(T), v_{\tilde{\nu}_i^c}(T)\}$, also find whatever metastable vacua $\vec{v}_{MS,i}$ are near to $\vec{x}_{n_1 n_2 n_3}$ and $\vec{y}_{n_1 n_2 n_3}$, as the temperature increases the location and depth of these stationary points will change, converge on the critical temperature T_c at which the EWSB vacuum becomes degenerate with one of the EW-preserving minima $V_{\text{eff}}^{T_c}(\vec{v}_{EWSB}(T_c)) = V_{\text{eff}}^{T_c}(\vec{v}_{MS,i^*}(T_c))$, compute $v(T_c) = \sqrt{|v_1(T_c)|^2 + |v_2(T_c)|^2}$ as the Higgs VEV in the broken phase. Using this procedure, we obtain T_c and $v(T_c)$ for the lowest temperature phase transition. Generally in this region of parameter space, multiple phase transition steps are required to bring the field configuration from the high-temperature symmetric phase to the zero temperature broken phase. We must investigate separately earlier steps.

The results of the 2000 point parameter space scan are summarized in Figure 5 where regions IIIa and IIIb are the only likely viable regions for SFOPT EWBG. We will describe the different regions here and give an analytic derivation of the boundaries and their parametric dependence in Appendix C. The points in region I are excluded because the EWSB vacuum, where $v(0) = 174$ GeV, contains a tachyonic direction. The points in region II are excluded because the EWSB vacuum is metastable. For regions IIa,b,c, the actual vacuum can be found at the following points: the origin of field space in region IIa, nearby to x_{012} in region IIb, and nearby to y_{012} in region IIc. That is, in regions IIa and IIb, the electroweak phase transition does not occur. Region IIc does not work for EWBG as well as we will see below. In region III there are no tachyons, no false minima, and all phenomenological mass bounds are satisfied, but as we will see only IIIa and IIIb are likely to give acceptable phase transitions for EWBG.

The phase transition at each point can be classified into one of four types based on the path that the vacuum follows through the $\{H_1^0, H_2^0, \tilde{\nu}_i^c\}$ field space. In the largest region IIIa, the PT makes two steps: from the origin to a $\{\text{EW}, \mathbb{Z}_3, \mathbb{S}_3, \text{CP}\}$ phase and then to the $\{\text{EW}, \mathbb{Z}_3, \mathbb{S}_3, \text{CP}\}$ phase. In region IIIb the EWPT occurs in one step directly from the

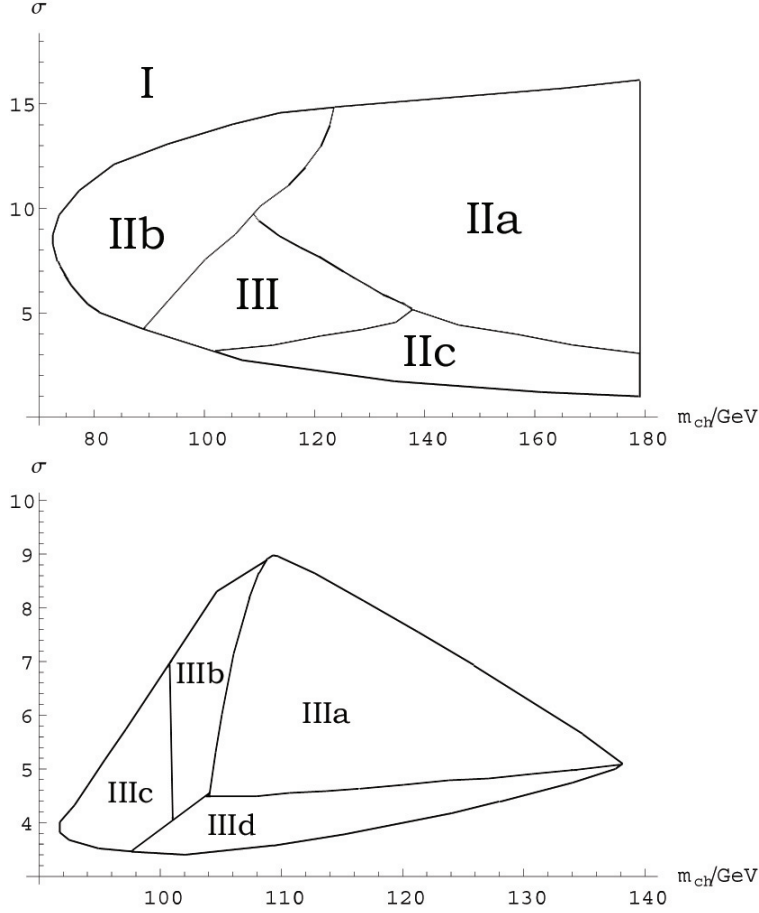


Figure 5: A slice of the $\mu\nu$ SSM parameter space. Region I suffers from tachyons in the EWSB vacuum. In region II the EWSB vacuum is metastable and we exclude these points. In region III we calculate the electroweak phase transition and find that the path through field space can be classified into one of four types, shown on the right.

origin to the EW-broken phase. In region IIIc, the EW symmetry is broken by a second order phase transition in which only H_2^0 gets a VEV; then, a first order phase transition occurs giving the singlets VEVs. Finally in region IIIId the phase transitions occur in three or four steps and there are multiple EWSB phases, whose details for a representative point are discussed below. However, as we will see, region IIIId is unlikely to give an acceptable EWBG scenario.

To understand how the $\mu\nu$ SSM phase transition differs from the NMSSM scenario, we have taken one representative parameter point from each sector of region III and followed the full phase transition from the origin \vec{x}_O to the zero temperature EWSB vacuum \vec{y}_{000} . In the tables, the minima above and below an arrow are degenerate at the temperature indicated. A 0^+ indicates that a second order phase transition occurs along the specified field direction.

IIIa. Two Step Transition via EW-preserving Phase: $\vec{x}_O \xrightarrow{1PT} \vec{x}_{012} \xrightarrow{1PT} \vec{y}_{000}$
 Representative point: $\{m_{\text{ch}}, \sigma\} = \{108.8 \text{ GeV}, 9.12\}$.

T	$\{H_1^0, H_2^0, \tilde{\nu}_i^c\}$ (GeV)	$\sqrt{2} \frac{v(T)}{T}$	Symmetries
$\gg M_w$	$\{0, 0, 0, 0, 0\}$	0	$\{\text{EW}, \mathbb{Z}_3, \mathbb{S}_3, \text{CP}\}$
$\xrightarrow{75.1 \text{ GeV}}$	$\{0, 0, 191.7, 191.7e^{i2\pi/3}, 191.7e^{i4\pi/3}\}$	0	$\{\text{EW}, \mathbb{Z}_3, \mathbb{S}_3, \text{CP}\}$
$\xrightarrow{54.6 \text{ GeV}}$	$\{0, 0, 192.6, 192.6e^{i2\pi/3}, 192.6e^{i4\pi/3}\}$ $\{61.7, 160.7, 201.0, 201.0, 201.0\}$	0 4.46	$\{\text{EW}, \mathbb{Z}_3, \mathbb{S}_3, \text{CP}\}$ $\{\text{EW}, \mathbb{Z}_3, \mathbb{S}_3, \text{CP}\}$
0 GeV	$\{62.5, 162.5, 201.5, 201.5, 201.5\}$	N/A	$\{\text{EW}, \mathbb{Z}_3, \mathbb{S}_3, \text{CP}\}$

Table I: Phase transition path for the representative point in region IIIa.

At $T = 75.1$ GeV, a first order phase transition gives the singlets VEVs and breaks $\mathbb{Z}_3, \mathbb{S}_3$, and CP. The EW symmetry is broken by a strongly first order phase transition at 54.6 GeV which also restores \mathbb{S}_3 and CP. Baryon number may be generated at the strongly first order EW-breaking PT because sphalerons are suppressed by $\sqrt{2}v(T_c)/T_c = 4.46$ inside the bubble.

IIIb. One Step: $\vec{x}_O \xrightarrow{1PT} \vec{y}_{000}$

Representative point: $\{m_{\text{ch}}, \sigma\} = \{102.5 \text{ GeV}, 7.22\}$.

T	$\{H_1^0, H_2^0, \tilde{\nu}_i^c\}$	$\sqrt{2} \frac{v(T)}{T}$	Symmetries
$\gg M_w$	$\{0, 0, 0, 0, 0\}$	0	$\{\text{EW}, \mathbb{Z}_3, \mathbb{S}_3, \text{CP}\}$
$\xrightarrow{69.6 \text{ GeV}}$	$\{60.3, 157.7, 188.3, 188.3, 188.3\}$	3.43	$\{\text{EW}, \mathbb{Z}_3, \mathbb{S}_3, \text{CP}\}$
0 GeV	$\{62.5, 162.5, 189.8, 189.8, 189.8\}$	N/A	$\{\text{EW}, \mathbb{Z}_3, \mathbb{S}_3, \text{CP}\}$

Table II: Phase transition path for the representative point in region IIIb.

At $T = 69.6$ GeV, the Higgs and singlets obtain VEVs simultaneously breaking the EW symmetry and \mathbb{Z}_3 . This one step phase transition resembles the ones seen in certain parametric regions of the NMSSM and other Higgs-singlet extensions. A baryon number may be generated since $\sqrt{2}v(T_c)/T_c = 3.43$ in the broken phase will suppress washout. For the parameters in region IIIb, we have plotted in Figure 6 the order parameter and critical temperature as functions of $E_{\text{eff}}/(\lambda_{\text{eff}}\phi(0))$ which we calculate using the tree-level potential along the trajectory that joins \vec{x}_O and \vec{y}_{000} . The order parameter grows and the critical temperature decreases as $E_{\text{eff}}/(\lambda_{\text{eff}}\phi(0))$ approaches 1/2 from below. The data points do not extend all the way to 1/2 because the radiative corrections lift the potential in such a way that parameter sets with $E_{\text{eff}}/(\lambda_{\text{eff}}\phi(0)) \approx 1/2$ at tree-level have a metastable EWSB vacuum at one-loop.

IIIc. Two Step via EWSB Phase: $\vec{x}_O \xrightarrow{2PT} \vec{y}_{H_2} \xrightarrow{1PT} \vec{y}_{000}$

Representative point: $\{m_{\text{ch}}, \sigma\} = \{95.1 \text{ GeV}, 5.37\}$.

At a high temperature $T = 116.4$ GeV the EW symmetry is broken by a second order phase transition along the up-type Higgs direction. As the temperature decreases, the global minimum of the effective potential moves along the H_2^0 axis until it becomes degenerate with a minimum localized near to \vec{y}_{000} . A first order phase transition occurs

T	$\{H_1^0, H_2^0, \tilde{\nu}_i^c\}$	$\sqrt{2} \frac{v(T)}{T}$	Symmetries
$\gg M_w$	$\{0, 0, 0, 0, 0\}$	0	$\{\text{EW}, \mathbb{Z}_3, \mathbb{S}_3, \text{CP}\}$
$\xrightarrow{116.4 \text{ GeV}}$	$\{0, 0^+, 0, 0, 0\}$	0^+	$\{\text{E}\cancel{\text{W}}, \mathbb{Z}_3, \mathbb{S}_3, \text{CP}\}$
$\xrightarrow{57.6 \text{ GeV}}$	$\{0, 101, 0, 0, 0\}$	2.5	$\{\text{E}\cancel{\text{W}}, \mathbb{Z}_3, \mathbb{S}_3, \text{CP}\}$
	$\{61.6, 160.6, 175.4, 175.4, 175.4\}$	4.25	$\{\text{E}\cancel{\text{W}}, \mathbb{Z}_3, \mathbb{S}_3, \text{CP}\}$
0 GeV	$\{62.5, 162.5, 176.2, 176.2, 176.2\}$	N/A	$\{\text{E}\cancel{\text{W}}, \mathbb{Z}_3, \mathbb{S}_3, \text{CP}\}$

Table III: Phase transition path for the representative point in region IIIc.

with $\sqrt{2}v(T_c)/T_c = 4.25$ inside the bubble and $\sqrt{2}v(T_c)/T_c = 2.5$ outside the bubble. In this scenario, there is no baryon number generation. Because the first transition is of the second order, there is no coexistence of phases. The second transition is first order, but the sphaleron transition rate is suppressed both inside and outside the bubble such that $B + L$ is preserved on both sides.

IIIId. Multi-Step: $\vec{x}_O \xrightarrow{1PT} \vec{x}_{012} \xrightarrow{1PT} (\vec{y}_{001} \text{ or } \vec{y}_{002}) \xrightarrow{1PT} \vec{y}_{000}$
 Representative point: $\{m_{\text{ch}}, \sigma\} = \{121.6 \text{ GeV}, 4.40\}$.

T	$\{H_1^0, H_2^0, \tilde{\nu}_i^c\}$	$\sqrt{2} \frac{v(T)}{T}$	Symmetries
$\gg M_w$	$\{0, 0, 0, 0, 0\}$	0	$\{\text{EW}, \mathbb{Z}_3, \mathbb{S}_3, \text{CP}\}$
$\xrightarrow{222.3 \text{ GeV}}$	$\{0, 0, 197, 197e^{i2\pi/3}, 197e^{i4\pi/3}\}$	0	$\{\text{EW}, \mathbb{Z}_3, \mathbb{S}_3, \text{CP}\}$
$\xrightarrow{128 \text{ GeV}}$	$\{0, 0, 229, 229e^{i2\pi/3}, 229e^{i4\pi/3}\}$	0	$\{\text{EW}, \mathbb{Z}_3, \mathbb{S}_3, \text{CP}\}$
	$\{0^+, 0^+, 229, 229e^{i2\pi/3}, 229e^{i4\pi/3}\}$	0^+	$\{\text{E}\cancel{\text{W}}, \mathbb{Z}_3, \mathbb{S}_3, \text{CP}\}$
$\xrightarrow{105 \text{ GeV}}$	$\{0^+, 82, 232, 232e^{i2\pi/3}, 232e^{i4\pi/3}\}$	1.1	$\{\text{E}\cancel{\text{W}}, \mathbb{Z}_3, \mathbb{S}_3, \text{CP}\}$
	$\{29e^{i1.9\pi}, 117e^{i1.9\pi}, 229, 229, 232e^{i2\pi/3}\}$	1.6	$\{\text{E}\cancel{\text{W}}, \mathbb{Z}_3, \mathbb{S}_3, \text{CP}\}$
$\xrightarrow{89.0 \text{ GeV}}$	$\{32.0, 128.0, 230.3, 230.3, 232.7e^{i2\pi/3}\}$	2.10	$\{\text{E}\cancel{\text{W}}, \mathbb{Z}_3, \mathbb{S}_3, \text{CP}\}$
	$\{58.4, 152.3, 224.4, 224.4, 224.4\}$	2.59	$\{\text{E}\cancel{\text{W}}, \mathbb{Z}_3, \mathbb{S}_3, \text{CP}\}$
0 GeV	$\{62.5, 162.5, 225.1, 225.1, 225.1\}$	N/A	$\{\text{E}\cancel{\text{W}}, \mathbb{Z}_3, \mathbb{S}_3, \text{CP}\}$

Table IV: Phase transition path for the representative point in region IIIId.

At this parametric point, the phase transition occurs in four steps with the EW symmetry broken in the second step by a second order phase transition. As the temperature drops from 128 GeV to 105 GeV, the sphaleron becomes increasingly suppressed. When the 1PT occurs at 105 GeV, the sphaleron is inactive, such that there will be no B-number generation. Not every phase transition in region IIIId follows this particular PT path, but the PTs are generally multi-step with at least one EWSB intermediate phase and transitional CP violation.

To give an impression of the particle masses in this region of parameter space, we include here the spectrum for the representative point in region IIIb where $\{m_{\text{ch}}, \sigma\} = \{102.5 \text{ GeV}, 7.22\}$. The slepton, squark, gaugino, and left-handed sneutrino masses are all $\mathcal{O}(\text{TeV})$ because we have fixed the soft masses in these sectors at a fiducial SUSY-breaking

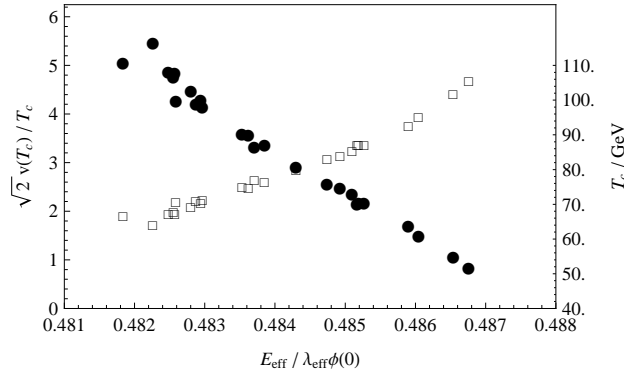


Figure 6: The order parameter (squares) and critical temperature (circles) plotted against $E_{\text{eff}}/\lambda_{\text{eff}}\phi(0)$ for the points in parametric region IIIb. We calculate $E_{\text{eff}}/\lambda_{\text{eff}}\phi(0)$ using the tree-level potential along the trajectory that connects the origin \vec{x}_O and zero temperature vacuum \vec{y}_{000} .

scale. In the case of the $\tilde{\nu}$, we solve for the soft mass using the minimization equations to find $m_L^2 \approx -a_\nu v_{\tilde{\nu}^c} v_2 / v_{\tilde{\nu}}$, yet it is still typically TeV scale because $A_\nu = a_\nu / Y_\nu = -1$ TeV. The remaining fermion and charged scalar spectrum is given by

$$\begin{aligned}
 m_{H^\pm} &= 342 \text{ GeV} \\
 m_{\tilde{H}^\pm} &= 96 \text{ GeV} \\
 m_{\nu^c} &= 260, 243, 243 \text{ GeV} \\
 m_{\tilde{\chi}_{1,2}^0} &= 88.7, 94.5 \text{ GeV, mostly Higgsino} \\
 m_\nu &= 41, 41, 7.8 \text{ meV}
 \end{aligned} \tag{50}$$

which are calculated at tree-level. The LSP is a Higgsino with mass 88.7 GeV. The degeneracies present in the neutrino sector result from the \mathbb{S}_3 symmetry of our Lagrangian. By allowing the left-handed sneutrinos to have different VEVs or choosing different values for the Y_ν Yukawas, we could obtain a correct neutrino hierarchy. We include these masses here to demonstrate that the seesaw matrix produces the correct mass scale for the light neutrinos. The neutral scalar masses are calculated at one-loop using the effective potential. Because there is significant mixing, we have included their mass eigenvalues and field composition in Table 5. Once again the degeneracies are a result of our \mathbb{S}_3 symmetry in the singlet sector. The lightest Higgs is mostly up-type with a mass of 110 GeV at this parametric point and only varies by 10 GeV over all of region III.

6. DOMAIN WALLS

It is well known [8, 49–53] that domain wall formation can be cosmologically problematic when spontaneous breaking of discrete symmetry occurs. In our scenario, we have only one “exact” discrete symmetry \mathbb{Z}_3 at the level of explicit parameterization of the Lagrangian. Because of the undesirable cosmological consequences of domain walls, we have implicitly assumed that this symmetry is broken by non-renormalizable operators which are cutoff by

Mass (GeV)	$\Re H_1^0$	$\Re H_2^0$	$\Re \tilde{\nu}_1^c$	$\Re \tilde{\nu}_2^c$	$\Re \tilde{\nu}_3^c$
395	0.83	0.16	0.00	0.00	0.00
140	0.01	0.21	0.26	0.26	0.26
128	0.00	0.00	0.58	0.01	0.41
128	0.00	0.00	0.09	0.65	0.07
110	0.16	0.63	0.07	0.07	0.07

Mass (GeV)	$\Im H_1^0$	$\Im H_2^0$	$\Im \tilde{\nu}_1^c$	$\Im \tilde{\nu}_2^c$	$\Im \tilde{\nu}_3^c$
439	0.48	0.07	0.15	0.15	0.15
369	0.00	0.00	0.02	0.39	0.59
369	0.00	0.00	0.65	0.27	0.08
314	0.39	0.06	0.18	0.18	0.18

Table V: CP-even and CP-odd Higgs masses and mixings for a sample parameter point. The field composition is described by the squared eigenvector associated with each eigenvalue.

a scale ⁸ larger than many TeV (such as not to disrupt the effective potential analysis). In addition, we have approximate discrete symmetries such as $\mathbb{S}_3 \otimes \text{CP}$ which a priori can cause problems if the symmetry breaking operators are overly suppressed. However, the set of electroweak symmetry breaking vacua of interest in this paper does not break $\mathbb{S}_3 \otimes \text{CP}$ (i.e. our symmetry breaking pattern can naturally select a $\mathbb{S}_3 \otimes \text{CP}$ singlet VEV to be the lowest energy vacuum as partly demonstrated in Appendix D). Hence, we will neglect any transient behavior and focus on \mathbb{Z}_3 domain walls even though the analysis is not very specific to the discrete group.⁹ Although a full analysis of domain wall histories is beyond the scope of this paper, here we briefly estimate the effects of the suppressed symmetry breaking operators that will alleviate the cosmological problems associated with domain walls that may form when the discrete symmetries considered in this paper are spontaneously broken. We will follow closely the work of Ref. [8].

In Ref. [8], it is estimated that during the approximate discrete symmetry breaking phase transition, domain walls separating approximately degenerate minima are formed. Then a simplified model of domain wall evolution is considered which approximately accounts for the surface tension of the bubble, the friction coming from bubble wall interaction with the plasma, and the pressure coming from energy density difference between the approximately degenerate minima. This last ingredient (pressure from energy density difference) is what will be coming from the inclusion of suppressed symmetry breaking operators, and we will refer to this simply as “pressure difference.” If the pressure difference dominates, one of the approximately degenerate phases will eat away at the higher energy phase regions and eventually dominate in a time scale controlled by the strength of the symmetry breaking operator.

Estimating the friction to be negligible, an approximate sufficient condition for curing the possible domain wall problem from a cosmological perspective is to have the pressure difference dominate before the equilibrium initial condition period of big bang nucleosynthesis: i.e. before the photon temperature reaches about 10 MeV. Explicitly, assuming order unity

⁸ Because we have $\lambda^2 + \kappa^2 < 0.5$ in the parametric regime of interest, the couplings should remain perturbative up to close to the GUT scale [14] (see e.g. [3] for explicit plots which suggest that our parametric choice is close to the border of perturbativity up to the GUT scale). Thus we are not severely restricted in the cutoff scale of our effective field theory.

⁹ For example, if one wanted to analyze transient domain walls associated with \mathbb{S}_3 breaking, one can easily work out from our Lagrangian the leading effective scalar operator breaking \mathbb{S}_3 and use the result at the end of this section.

Lorentz factor γ for the bubble wall speed, one must require

$$\epsilon > \frac{\sigma}{R(t)} \quad (51)$$

where ϵ is the energy density difference coming from suppressed symmetry breaking operators, σ is the energy per unit area of the bubble wall, and $R(t)$ is the time dependent radius of a typical bubble. For a dimension $4 + u$ non-derivative operator consisting of scalars only, ϵ can be estimated as

$$\epsilon \sim c_u \frac{v^{4+u}}{\Lambda^u} \quad (52)$$

where Λ is the cutoff scale and we have assumed all scalar VEVs to be of common order $v \equiv 174$ GeV (which is appropriate for our scenario). To be able to treat $u = 0$, we will set $\Lambda = 100$ TeV and find a bound on the value of c_u for different values of u . Assuming $R \sim t \sim 1/H$ (where H is the Hubble expansion rate) and $\sigma \sim v^3$, we find

$$c_u > 10^{-24} 500^u \quad (53)$$

for $u \geq 0$.¹⁰ Hence, as long as the cutoff is not required to be very large (in contrast with the assumption of Ref. [8]) or the accidental symmetry arising from the UV completion quantum numbers do not make u too large, this bound is very easy to satisfy for the \mathbb{Z}_3 domain wall problem. Of course, if the cutoff is taken to be high and/or a UV completion is desired without fine tuning, model building challenges along the lines of Refs. [9, 10] exist.

7. SUMMARY

We have uncovered a $\mu\nu$ SSM parametric region giving rise to a first order phase transition sufficiently strong to be useful for the electroweak baryogenesis scenarios involving electroweak symmetry breaking bubbles as the source of out of equilibrium and $SU(2)_L FF$ operators as a source of baryon number violation. The parametric region corresponds to tuning the soft terms in the Lagrangian $a_\lambda H_1 \cdot H_2 \tilde{\nu}_i^c$ and $-m_{\tilde{\nu}^c}^2 |\tilde{\nu}_i^c|^2$ to achieve Eq. (31). The numerical values of the uncovered parametric region is in the paragraph containing Eq. (46) and regions IIIa and IIIb depicted in Fig. 5. As expected, the Yukawa coupling of the singlets to the leptonic sector does not play a role in determining the strength of the phase transitions because of the weakness of the coupling tied to the smallness of the neutrino masses.

The region IIIa transitions are two-step transitions in which the electroweak symmetry breaking is the second transition that starts from a phase in which the singlet scalars of the $\mu\nu$ SSM have a non-zero vacuum expectation value (e.g. starts from a vacuum which spontaneously breaks the approximate S_3 symmetry in the singlet sector). These transitions contain a rotation in the singlet field space and do not have an analog in the NMSSM transitions because of the different dimensionality in the singlet complex vector space. The region IIIb transitions are the ones in which electroweak symmetry breaking transition starts from the origin of the scalar field space. All these transitions have useful descriptions in terms of the representations of the approximate discrete symmetries in the system.

¹⁰ This result can easily be checked to be consistent with Ref. [8] for $u = 1$.

Our phenomenological bounds were rather minimal and placed using Ref. [48], but in many parametric regions, the observables are sufficiently far away from the bounds that the plausibility of the phenomenological self-consistency is strong. Follow-up possibilities include a more complete collider related phenomenological investigation in this parametric regime, studies of domain wall histories due to weak global symmetry breaking operators, and a complete computation of CP asymmetry creation and transport leading to baryon asymmetry.

Given that the $\mu\nu$ SSM had to give up the popular thermal leptogenesis scenario due to its low scale implementation of the type I seesaw, this work is of interest as it shows that electroweak baryogenesis may be a promising avenue to create baryon asymmetry in this class of models. Given that the $\mu\nu$ SSM is one of the few supersymmetric models in which all dynamical degrees of freedom responsible for the neutrino mass may be accessible at TeV scale colliders, it is encouraging that the model has a good chance at being consistent with the observed baryon asymmetry in the universe.

Acknowledgments

We thank Amjad Ashoorioon, Lisa Everett, Aki Hashimoto, Carlos Muñoz, David Morrissey, and Michael Ramsey-Musolf for useful correspondence. We thank the hospitality of KIAS where part of this work was completed. This work is supported by the DOE through grant DE-FG02-95ER40896.

Appendix A: Field Dependent Mass Matrices

Here we include the tree-level, field dependent mass matrices which are required to compute the one-loop radiative corrections. We fix the charged scalars at their vanishing VEVs, let the left-handed sneutrino VEV $\tilde{\nu}_i = v_{\tilde{\nu}}$ be real, and treat the matrices as functions of the complex fields $\{H_1^0, H_2^0, \tilde{\nu}_i^c\}$.

Neutralinos. Using the basis $(\chi^0)^T = \{\tilde{B}, \tilde{W}_3, \tilde{H}_1^0, \tilde{H}_2^0, \nu_1^c, \nu_2^c, \nu_3^c, \nu_1, \nu_2, \nu_3\}$, the mass term appears as $\mathcal{L} \ni -\frac{1}{2}(\chi^0)^T M_{\chi^0}(\chi^0) + \text{h.c.}$ with $n_{\chi^0} = -2$ and

$$M_{\chi^0} = \begin{pmatrix} \mathcal{M} & m \\ m^T & 0_{3 \times 3} \end{pmatrix} \quad (\text{A1})$$

$$m^T = \begin{pmatrix} -\frac{g_1}{\sqrt{2}}v_{\tilde{\nu}} & \frac{g_2}{\sqrt{2}}v_{\tilde{\nu}} & 0 & Y_{\nu}\tilde{\nu}_1^c & Y_{\nu}H_2^0 & 0 & 0 \\ -\frac{g_1}{\sqrt{2}}v_{\tilde{\nu}} & \frac{g_2}{\sqrt{2}}v_{\tilde{\nu}} & 0 & Y_{\nu}\tilde{\nu}_2^c & 0 & Y_{\nu}H_2^0 & 0 \\ -\frac{g_1}{\sqrt{2}}v_{\tilde{\nu}} & \frac{g_2}{\sqrt{2}}v_{\tilde{\nu}} & 0 & Y_{\nu}\tilde{\nu}_3^c & 0 & 0 & Y_{\nu}H_2^0 \end{pmatrix} \quad (\text{A2})$$

and \mathcal{M} is a symmetric, sparse matrix with non-zero elements

$$\mathcal{M}_{\tilde{B}\tilde{B}} = M_1 \quad (\text{A3})$$

$$\mathcal{M}_{\tilde{B}\tilde{H}_1^0} = -\frac{g_1}{\sqrt{2}} (H_1^0)^* \quad (\text{A4})$$

$$\mathcal{M}_{\tilde{B}\tilde{H}_2^0} = \frac{g_1}{\sqrt{2}} (H_2^0)^* \quad (\text{A5})$$

$$\mathcal{M}_{\tilde{W}_3\tilde{W}_3} = M_2 \quad (\text{A6})$$

$$\mathcal{M}_{\tilde{W}_3\tilde{H}_1^0} = \frac{g_2}{\sqrt{2}} (H_1^0)^* \quad (\text{A7})$$

$$\mathcal{M}_{\tilde{W}_3\tilde{H}_2^0} = -\frac{g_2}{\sqrt{2}} (H_2^0)^* \quad (\text{A8})$$

$$\mathcal{M}_{\tilde{H}_1^0\tilde{H}_2^0} = -\lambda (\tilde{\nu}_1^c + \tilde{\nu}_2^c + \tilde{\nu}_3^c) \quad (\text{A9})$$

$$\mathcal{M}_{\tilde{H}_1^0\nu_i^c} = -\lambda H_2^0 \quad (\text{A10})$$

$$\mathcal{M}_{\tilde{H}_2^0\nu_i^c} = -\lambda H_1^0 + Y_\nu v_{\tilde{\nu}} \quad (\text{A11})$$

$$\mathcal{M}_{\nu_i^c\nu_j^c} = 2\kappa\tilde{\nu}_i^c\delta_{ij} \quad (\text{A12})$$

Charginos. Using the basis $(\Psi^+)^T = \{-i\tilde{\lambda}^+, \tilde{H}_2^+, e_R^+, \mu_R^+, \tau_R^+\}$ and $(\Psi^-)^T = \{-i\tilde{\lambda}^-, \tilde{H}_1^-, e_L^-, \mu_L^-, \tau_L^-\}$ the mass term appears as $\mathcal{L} \ni -\frac{1}{2}(\Psi^-)^T M_{\chi^\pm} (\Psi^+) + \text{transpose}$ with $n_{\chi^\pm} = -2$ and

$$M_{\chi^\pm} = \begin{pmatrix} M_2 & g_2 (H_2^0)^* & 0 & 0 & 0 \\ g_2 (H_1^0)^* & \lambda (\tilde{\nu}_1^c + \tilde{\nu}_2^c + \tilde{\nu}_3^c) & -Y_e v_{\tilde{\nu}} & -Y_\mu v_{\tilde{\nu}} & -Y_\tau v_{\tilde{\nu}} \\ g_2 v_{\tilde{\nu}} & -Y_\nu \tilde{\nu}_1^c & Y_e H_1^0 & 0 & 0 \\ g_2 v_{\tilde{\nu}} & -Y_\nu \tilde{\nu}_2^c & 0 & Y_\mu H_1^0 & 0 \\ g_2 v_{\tilde{\nu}} & -Y_\nu \tilde{\nu}_3^c & 0 & 0 & Y_\tau H_1^0 \end{pmatrix}. \quad (\text{A13})$$

Gauge Bosons. The propagators and field dependent masses in the gauge sector have gauge dependence. We work in the Landau gauge ($\xi = 0$), in which the scalar component and ghost propagators have no field dependence. The charged gauge bosons have field dependent mass

$$M_{W^\pm}^2 = \frac{g_2^2}{2} \left(|H_1^0|^2 + |H_2^0|^2 + 3v_{\tilde{\nu}}^2 \right) \quad (\text{A14})$$

and in the basis $\{W_3, B\}$ the neutral gauge bosons have the mass matrix

$$M_{W_3 B}^2 = \begin{pmatrix} \frac{g_2^2}{2} \left(|H_1^0|^2 + |H_2^0|^2 + 3v_{\tilde{\nu}}^2 \right) & -\frac{g_1 g_2}{2} \left(|H_1^0|^2 + |H_2^0|^2 + 3v_{\tilde{\nu}}^2 \right) \\ -\frac{g_1 g_2}{2} \left(|H_1^0|^2 + |H_2^0|^2 + 3v_{\tilde{\nu}}^2 \right) & \frac{g_1^2}{2} \left(|H_1^0|^2 + |H_2^0|^2 + 3v_{\tilde{\nu}}^2 \right) \end{pmatrix}. \quad (\text{A15})$$

In order to count the degrees of freedom in the gauge sector, we must distinguish longitudinal and transverse components of the gauge boson fields, $2n_{W_L^\pm} = n_{W_T^\pm} = 4$ and $2n_{W_3 B_L} = n_{W_3 B_T} = 2$. We do this because only the longitudinal components receive thermal

mass corrections in the computation of the daisy correction Eq. (15), [54]. Note that $v_{\tilde{\nu}}^2$ is numerically negligible in these equations over all parameter regions of interest.

Squarks. Because we assume there is no inter-generational mixing in the squark sector, the squark mass matrix block diagonalizes. The i^{th} generation up- and down-type squarks have mass terms $\mathcal{L} \ni -\frac{1}{2}\tilde{q}_i^\dagger M_{\tilde{q}_i}^2 \tilde{q}_i$ in the basis $\tilde{q}_i = \{\tilde{q}_{L_i}, \tilde{q}_{R_i}^*\}$ with $n_q = 12$ and

$$(M_{\tilde{u}_i}^2)_{11} = M_Q^2 + \frac{1}{6} \left(\frac{3g_2^2}{2} - \frac{g_1^2}{2} \right) \left(|H_1^0|^2 - |H_2^0|^2 + 3v_{\tilde{\nu}}^2 \right) + Y_{u_i}^2 |H_2^0|^2 \quad (\text{A16})$$

$$(M_{\tilde{u}_i}^2)_{12} = (M_{\tilde{u}_i}^2)_{21}^* = a_u (H_2^0)^* - Y_{\nu} Y_u v_{\tilde{\nu}} (\tilde{\nu}_1^c + \tilde{\nu}_2^c + \tilde{\nu}_3^c) - Y_{u_i} \lambda (H_1^0) (\tilde{\nu}_1^c + \tilde{\nu}_2^c + \tilde{\nu}_3^c) \quad (\text{A17})$$

$$(M_{\tilde{u}_i}^2)_{22} = m_{\tilde{u}^c}^2 + \frac{g_1^2}{3} \left(|H_1^0|^2 - |H_2^0|^2 + 3v_{\tilde{\nu}}^2 \right) + Y_{u_i}^2 |H_2^0|^2 \quad (\text{A18})$$

$$(M_{\tilde{d}_i}^2)_{11} = M_Q^2 - \frac{1}{6} \left(\frac{3g_2^2}{2} + \frac{g_1^2}{2} \right) \left(|H_1^0|^2 - |H_2^0|^2 + 3v_{\tilde{\nu}}^2 \right) + Y_{d_i}^2 |H_1^0|^2 \quad (\text{A19})$$

$$(M_{\tilde{d}_i}^2)_{12} = (M_{\tilde{d}_i}^2)_{21}^* = a_d (H_1^0) - Y_{d_i} \lambda (H_2^0)^* (\tilde{\nu}_1^c + \tilde{\nu}_2^c + \tilde{\nu}_3^c)^* \quad (\text{A20})$$

$$(M_{\tilde{d}_i}^2)_{22} = m_{\tilde{d}^c}^2 - \frac{g_1^2}{6} \left(|H_1^0|^2 - |H_2^0|^2 + 3v_{\tilde{\nu}}^2 \right) + Y_{d_i}^2 |H_1^0|^2 \quad (\text{A21})$$

Charged Scalars. The charged Higgs mixes with the charged sleptons. Using the basis $S^+ = \{H_1^+, H_2^+, \tilde{e}_L^+, \tilde{e}_R^+, \tilde{\mu}_L^+, \tilde{\mu}_R^+, \tilde{\tau}_L^+, \tilde{\tau}_R^+\}$, the mass term is $\mathcal{L} \ni -S^+ M_{H^\pm}^2 S^-$ with $n_{H^\pm} = 2$ and the elements of the Hermitian mass matrix are

$$(M_{H^\pm}^2)_{H_1 H_1} = m_{H_1}^2 + v_{\tilde{\nu}}^2 \sum_{i=1}^3 Y_{e_i}^2 + \frac{1}{4} (g_1^2 + g_2^2) |H_1^0|^2 + \frac{1}{4} (g_1^2 - g_2^2) \left(3v_{\tilde{\nu}}^2 - |H_2^0|^2 \right) + \lambda^2 |\tilde{\nu}_1^c + \tilde{\nu}_2^c + \tilde{\nu}_3^c|^2 \quad (\text{A22})$$

$$(M_{H^\pm}^2)_{H_1 H_2} = a_\lambda \sum_{i=1}^3 \tilde{\nu}_i^c + 3v_{\tilde{\nu}} Y_\nu \lambda (H_2^0)^* + \left(\frac{1}{2} g_2^2 - 3\lambda^2 \right) (H_1^0 H_2^0)^* + \kappa \lambda \sum_{i=1}^3 (\tilde{\nu}_i^c)^{2*} \quad (\text{A23})$$

$$(M_{H^\pm}^2)_{H_2 H_2} = m_{H_2}^2 + \frac{1}{4} (g_1^2 + g_2^2) |H_2^0|^2 - \frac{1}{4} (g_1^2 - g_2^2) \left(3v_{\tilde{\nu}}^2 + |H_1^0|^2 \right) + Y_\nu^2 \sum_{i=1}^3 |\tilde{\nu}_i^c|^2 + \lambda^2 |\tilde{\nu}_1^c + \tilde{\nu}_2^c + \tilde{\nu}_3^c|^2 \quad (\text{A24})$$

$$(M_{H^\pm}^2)_{H_1 \tilde{\ell}_{L_i}} = \left(\frac{1}{2} g_2^2 - Y_{e_i}^2 \right) v_{\tilde{\nu}} (H_1^0)^* - Y_\nu \lambda (\tilde{\nu}_i^c)^* \sum_{k=1}^3 \tilde{\nu}_k^c \quad (\text{A25})$$

$$(M_{H^\pm}^2)_{H_1 \tilde{\ell}_{R_i}} = -a_{e_i} v_{\tilde{\nu}} - Y_\nu Y_{e_i} (H_2^0 \tilde{\nu}_i^c)^* \quad (\text{A26})$$

$$(M_{H^\pm}^2)_{H_2 \tilde{\ell}_{L_i}} = \left(\frac{1}{2} g_2^2 - Y_\nu^2 \right) v_{\tilde{\nu}} H_2^0 + \lambda Y_\nu H_1^0 H_2^0 - Y_\nu \kappa (\tilde{\nu}_i^c)^2 - a_\nu (\tilde{\nu}_i^c)^* \quad (\text{A27})$$

$$(M_{H^\pm}^2)_{H_2 \tilde{\ell}_{R_i}} = -Y_\nu Y_{e_i} H_1^0 (\tilde{\nu}_i^c)^* - \lambda Y_{e_i} v_{\tilde{\nu}} \sum_{k=1}^3 (\tilde{\nu}_k^c)^* \quad (\text{A28})$$

$$(M_{H^\pm}^2)_{\tilde{\ell}_{L_i} \tilde{\ell}_{L_j}} = \delta_{ij} \left[m_L^2 + \frac{1}{4} (g_1^2 - g_2^2) (|H_1^0|^2 - |H_2^0|^2 + 3v_{\tilde{\nu}}^2) + Y_{e_i}^2 |H_1^0|^2 \right] + \frac{1}{2} g_2^2 v_{\tilde{\nu}}^2 + Y_\nu^2 \tilde{\nu}_i^c (\tilde{\nu}_j^c)^* \quad (\text{A29})$$

$$(M_{H^\pm}^2)_{\tilde{\ell}_{R_i} \tilde{\ell}_{R_j}} = \delta_{ij} \left[m_{ec}^2 - \frac{1}{2} g_1^2 (|H_1^0|^2 - |H_2^0|^2 + 3v_{\tilde{\nu}}^2) + Y_{e_i}^2 |H_1^0|^2 \right] + Y_{e_i} Y_{e_j} v_{\tilde{\nu}}^2 \quad (\text{A30})$$

$$(M_{H^\pm}^2)_{\tilde{\ell}_{L_i} \tilde{\ell}_{R_j}} = \delta_{ij} \left[a_{e_i} H_1^0 - \lambda Y_{e_i} (H_2^0)^* \sum_{k=1}^3 (\tilde{\nu}_k^c)^* \right] . \quad (\text{A31})$$

Neutral Scalars. The neutral Higgses mix with the left- and right-handed sneutrinos in a 16×16 matrix $M_{H_0}^2$. At the EWSB vacuum which respects CP, this matrix block diagonalizes into CP-even and CP-odd sectors. In order to study the phase transition in which there are transitional CP-violating phases, we must retain the off-diagonal blocks. In the basis $\phi^T = \{\Re H_0, \Im H_0\}$ where $H_0 = \{H_1^0, H_2^0, \tilde{\nu}_1^c, \tilde{\nu}_2^c, \tilde{\nu}_3^c, \tilde{\nu}_1, \tilde{\nu}_2, \tilde{\nu}_3\}$ the mass term is given by $\mathcal{L} \ni -\frac{1}{2} \phi^T M_{H_0}^2 \phi$ with $n_{H_0} = 1$. One can obtain the mass matrix

$$(M_{H_0}^2)_{ij} = \begin{pmatrix} M_{\Re H_0}^2 & M_{C/P}^2 \\ M_{C/P}^2 & M_{\Im H_0}^2 \end{pmatrix}_{ij} = \frac{\partial^2 \bar{V}_0}{\partial \phi_i \partial \phi_j} . \quad (\text{A32})$$

by differentiating the full scalar potential

$$\begin{aligned} \bar{V}_0 = & V_0 + m_L^2 \sum_i |\tilde{\nu}_i|^2 + Y_\nu^2 \left(|H_2^0|^2 \sum_i |\tilde{\nu}_i|^2 + \left| \sum_i \tilde{\nu}_i \tilde{\nu}_i^c \right|^2 \right) \\ & + \sum_i [a_\nu H_2^0 \tilde{\nu}_i \tilde{\nu}_i^c + Y_\nu \kappa (H_2^0 \tilde{\nu}_i)^* (\tilde{\nu}_i^c)^2 + \text{h.c.}] \\ & - \lambda Y_\nu \sum_i \left[|H_2^0|^2 H_1^0 \tilde{\nu}_i^* + H_1^0 \tilde{\nu}_i^c \sum_j (\tilde{\nu}_j \tilde{\nu}_j^c)^* + \text{h.c.} \right] \\ & + \left[\frac{g_1^2 + g_2^2}{8} \left(|H_1^0|^2 - |H_2^0|^2 + \sum_i |\tilde{\nu}_i|^2 \right)^2 - \frac{g_1^2 + g_2^2}{8} \left(|H_1^0|^2 - |H_2^0|^2 \right)^2 \right] \end{aligned} \quad (\text{A33})$$

where the dominant contribution V_0 is given by Eq. (9).

Appendix B: Bosonic Thermal Masses

In order to calculate the daisy resummation Eq. (15) we require the thermal mass corrections Π_b . For the Higgs and singlet fields we compute the thermal mass corrections from the thermal effective potential using the procedure explained in this section. For the left-handed sneutrinos we use

$$\frac{\Pi_{\tilde{\nu}_i}}{T^2} = \frac{g_1^2}{8} + \frac{7g_2^2}{24} + \frac{5Y_{e_i}^2}{24} + \frac{Y_\nu^2}{4} \quad (\text{B1})$$

which can be calculated by assuming that all species that are summed in ΔV_1^T are light. For the remaining bosonic species, we use the thermal mass functions calculated for the nMSSM by [12] in which the authors assumed that the Higgs, Higgsinos, electroweak gauginos, and SM particles were light.

First, we evaluate the thermal effective potential correction Eq. (13) as a function of the eigenvalues of the field dependent mass matrices listed in Appendix A. Let \tilde{m}_{ij}^2 be the j^{th} eigenvalue of the i^{th} mass matrix with has n_i associated degrees of freedom. By writing the traces as a sum over eigenvalues and using that $n_i < 0$ for fermionic species, Eq. (13) can be written as

$$\Delta V_1^T = \frac{T^4}{2\pi^2} \sum_i |n_i| \begin{cases} \sum_j J_B(\tilde{m}_{ij}^2/T^2) & \text{i bosonic} \\ -\sum_j J_F(\tilde{m}_{ij}^2/T^2) & \text{i fermionic} \end{cases}. \quad (\text{B2})$$

In the high-temperature limit, $\tilde{m}_{ij}^2 \ll T^2$ the bosonic and fermionic thermal functions can be expanded as

$$J_B(y) \xrightarrow{y \ll 1} \frac{\pi^2}{12} y + \mathcal{O}(y^{3/2}) \quad (\text{B3})$$

$$J_F(y) \xrightarrow{y \ll 1} -\frac{\pi^2}{24} y + \mathcal{O}(y^2) \quad (\text{B4})$$

plus field independent terms. Second, we define the high-temperature thermal potential correction by imposing a sharp cutoff at $\tilde{m}_{ij}^2 = 2T^2$ to obtain

$$\Delta V_1^{T,\text{high}} = \frac{1}{48} T^2 \sum_i |n_i| \begin{cases} \sum_j 2\tilde{m}_{ij}^2 & \text{i bosonic} \\ \sum_j \tilde{m}_{ij}^2 & \text{i fermionic} \\ 0 & \tilde{m}_{ij}^2 < 2T^2 \end{cases} \quad (\text{B5})$$

Third, we extract the thermal mass corrections by differentiating with respect to the Higgs and singlet fields,

$$\Pi_{\phi_i} = T^2 \left[\frac{\partial^2}{\partial \phi_i^2} \frac{\Delta V_1^{T,\text{high}}}{T^2} \right]_{H_1^0=H_2^0=\tilde{\nu}_k^c=0, T=100 \text{ GeV}} \quad (\text{B6})$$

where $\phi_i \in \{H_1^0, H_2^0, \tilde{\nu}_k^c\}$. The derivatives are evaluated at the origin in field space such that Π_{ϕ_i} is accurate in the high-temperature vacuum. Because the derivative in Eq. (B6) has only weak field dependence, we expect this expression for Π_{ϕ_i} to be accurate even for our multi-step phase transitions in which the singlets have VEVs before the EWPT. The value of T used in Eq. (B6) only affects the location of the cutoff in Eq. (B5). We have chosen the temperature $T = 100$ GeV to be at the appropriate scale for our phase transitions and such that Π_{ϕ_i} does not vary discontinuously in the region of parameter space with first order phase transitions. Using this procedure we obtain $\Pi_{H_1^0} \approx 0.11 T^2$, $\Pi_{H_2^0} \approx 0.40 T^2$, $\Pi_{\tilde{\nu}_k^c} \approx 0.20 T^2$ over the region of parameter space with phase transitions.

Appendix C: Analytic Derivation of Parameter Space Boundaries

The boundaries in Figure 5 can be understood analytically. In this section, we derive expressions for each of the boundaries and discuss the parametric dependence.

At the interface of regions I and II, the electroweak vacuum develops a tachyonic direction at tree-level and $\det M_{\mathfrak{R}H_0}^2 = 0$. Since $M_{\mathfrak{R}H_0}^2$ is an 8 by 8 matrix, it would not be useful to write out its determinant. Instead, we observe that the tachyonic direction is directed along $\{H_1^0/v_1, H_2^0/v_2, \tilde{\nu}_i^c/v_{\tilde{\nu}^c} \approx 1, \tilde{\nu}_i = 0\}$.

At the boundary between region IIa and III, the minima at \vec{x}_{012} and \vec{y}_{000} are degenerate at one-loop. Note that this degeneracy cannot occur at tree-level. To see why, write

$$V_0(\vec{x}_{012}) - V_0(\vec{y}_{000}) = \Delta V_0^a + \Delta V_0^b \quad (\text{C1})$$

with $\Delta V_0^a = V_0(\vec{x}_{012}) - V_0(\vec{x}_{000})$ and $\Delta V_0^b = V_0(\vec{x}_{000}) - V_0(\vec{y}_{000})$. The tree-level $(\mathbb{Z}_3)^3$ symmetry ensures $\Delta V_0^a = 0$. Additionally, the minimization equations Eq. (10) require that the potential has a minimum at \vec{y}_{000} . Therefore, we have

$$\Delta V_0^b = \frac{1}{8} [(g_1^2 + g_2^2) \cos^2 2\beta + 6\lambda^2 \sin^2 2\beta] v^4 > 0. \quad (\text{C2})$$

At one-loop order we calculate the difference in the potential as

$$V_1^0(\vec{x}_{012}) - V_1^0(\vec{y}_{000}) = \Delta V_1^a + \Delta V_1^b \quad (\text{C3})$$

where V_1^0 is the one-loop, zero temperature effective potential and $\Delta V_1^{a,b}$ are defined analogously as above. We expect ΔV_1^a to be nonzero and sensitive to the radiative corrections because the $(\mathbb{Z}_3)^3$ symmetry is broken to \mathbb{Z}_3 . The terms responsible for this symmetry breaking are the superpotential term $W \ni \lambda \hat{H}_1^0 \hat{H}_2^0 \hat{\nu}_i^c$ and corresponding A-term in the soft SUSY-breaking Lagrangian. We calculate

$$64\pi^2 \Delta V_1^a = 6m_{\text{ch}}^4 \log \frac{m_{\text{ch}}^2}{e^{3/2}\mu^2} + 4 \left[m_{H_1}^4 \log \frac{m_{H_1}^2}{e^{3/2}\mu^2} + m_{H_2}^4 \log \frac{m_{H_2}^2}{e^{3/2}\mu^2} - \sum_{\pm} m_{\pm}^4 \log \frac{m_{\pm}^2}{e^{3/2}\mu^2} \right]$$

$$m_{\pm}^2 = m_{\text{ch}}^2 + \frac{m_{H_1}^2 + m_{H_2}^2}{2} \pm \frac{1}{2} \sqrt{(m_{H_1}^2 - m_{H_2}^2)^2 + \sigma^2 m_{\text{ch}}^4} \quad (\text{C4})$$

For the sake of discussion, we can approximate the logarithms in the second term as order one numbers and eliminate the soft masses using Eq. (10) to obtain

$$64\pi^2 \Delta V_1^a \approx 6m_{\text{ch}}^4 \log \frac{m_{\text{ch}}^2}{e^{3/2}\mu^2} - 2m_{\text{ch}}^4 (\sigma^2 + 4\sigma \csc 2\beta - 4) + 24\lambda^2 v^2 m_{\text{ch}}^2 \quad (\text{C5})$$

Since we are simply trying to estimate the parametric dependence, we can approximate $\Delta V_1^b \approx \Delta V_0^b$. By requiring that the minimum at \vec{x}_{012} is not deeper than the EWSB vacuum, we obtain the bound $\Delta V_1^a + \Delta V_0^b \geq 0$, which is saturated at the interface of regions IIa and III. This bound disfavors large m_{ch} and large σ because of the $-m_{\text{ch}}^4 \sigma^2$ term in ΔV_1^a .

At the boundary where regions III and IIa meet, the EWSB is degenerate with the origin in field space at one-loop. Neglecting the radiative corrections we can approximate the splitting as $V_1^0(\vec{x}_O) - V_1^0(\vec{y}_{000}) \approx V_0(\vec{x}_O) - V_0(\vec{y}_{000}) \equiv \Delta V_0^c$ with

$$\Delta V_0^c = \frac{1}{8} [(g_1^2 + g_2^2) \cos^2 2\beta + 6\lambda^2 \sin^2 2\beta] v^4$$

$$+ m_{\text{ch}}^2 v^2 \left[1 - \frac{\kappa \sin 2\beta}{6\lambda} - \frac{\sigma \sin 2\beta}{4} \right] + \frac{m_{\text{ch}}^4 \kappa^2}{27\lambda^4} + \frac{a_{\kappa} m_{\text{ch}}^3}{27\lambda^3} \quad (\text{C6})$$

To prevent the origin from becoming the global minimum we require $\Delta V_0^c > 0$ which favors larger m_{ch} and smaller σ .

At the boundary between regions IIc and III, the one-loop potential has degenerate minima at \vec{y}_{012} and \vec{y}_{000} . We can compute the splitting $\Delta V_0^d \equiv V_0(\vec{y}_{012}) - V_0(\vec{y}_{000})$ by neglecting the radiative corrections to find

$$\Delta V_0^d = \frac{1}{2} m_{\text{ch}}^2 v^2 (\sigma \sin 2\beta - 2). \quad (\text{C7})$$

The condition that the EWSB minimum at \vec{y}_{000} is absolutely stable requires $\Delta V_0^d > 0$ which imposes the lower bound $\sigma \gtrsim 2 \csc 2\beta \approx 3$ for $\tan \beta = 2.6$. Figure 5 shows that the IIc-III boundary also depends on m_{ch} contrary to Eq. (C7), but this is a result of the radiative corrections.

Appendix D: Selecting a CP-Even Vacuum

In this Appendix, we show formally how a superpotential contribution ΔW that breaks \mathbb{Z}_3 weakly can be constructed to make the CP conserving vacuum to have the lowest energy perturbatively in the absence of any explicit CP violating parameters. Consider the superpotential

$$W = W_0 + \Delta W \quad (\text{D1})$$

where ΔW represents a irrelevant operator perturbation to renormalizable W_0 . We then have

$$\sum_i \left| \frac{\partial W}{\partial \phi_i} \right|^2 = \sum_i \left\{ \left| \frac{\partial W_0}{\partial \phi_i} \right|^2 + 2\Re \left[\left(\frac{\partial \Delta W}{\partial \phi_i} \right) \left(\frac{\partial W_0}{\partial \phi_i} \right)^* \right] \right\} \quad (\text{D2})$$

$$= V_0 + \sum_i \Delta V_i \quad (\text{D3})$$

where

$$V_0 \equiv \sum_i \left| \frac{\partial W_0}{\partial \phi_i} \right|^2 \quad (\text{D4})$$

and

$$\Delta V_i \equiv 2\Re \left[\left(\frac{\partial \Delta W}{\partial \phi_i} \right) \left(\frac{\partial W_0}{\partial \phi_i} \right)^* \right] \quad (\text{D5})$$

to leading order in ΔW which we will call $\mathcal{O}(\delta)$. As usual, W_0 and ΔW are holomorphic polynomials in fields. Considering $\phi_i \rightarrow \phi_i^*$ as a representation of \mathbb{Z}_2 which we will call 2, we have

$$\left(\frac{\partial \Delta W}{\partial \phi_i} \right) \left(\frac{\partial W_0}{\partial \phi_i} \right)^* \quad (\text{D6})$$

being a representation of

$$\oplus \sum_u (2^u \otimes \bar{2}^2) \equiv R. \quad (\text{D7})$$

If we assume all the coefficients of W and ΔW are real, we can write

$$2\Re \left[\left(\frac{\partial \Delta W}{\partial \phi_i} \right) \left(\frac{\partial W_0}{\partial \phi_i} \right)^* \right] = R \oplus \mathbb{Z}_2(R) \quad (\text{D8})$$

where $\mathbb{Z}_2(\mathbb{Z}_2(R)) = R$. Hence, we see that ΔV_i is a singlet under \mathbb{Z}_2 . Given that ΔV_i is a polynomial in $a_j \equiv \Re \phi_j$ and $b_j \equiv \Im \phi_j$ and since under $\mathbb{Z}_2 : \{a_j \rightarrow a_j, b_j \rightarrow -b_j\}$, we must have

$$\Delta V_i = \sum_k \sum_m c_{km}^i P_k(\{a_j\}) S_m(\{b_j\}) \quad (\text{D9})$$

where S_m represents a basis of \mathbb{Z}_2 singlet polynomial functions composed of b_j and P_k is a basis of polynomial functions composed of a_j . Note that here $c_{km}^i = \mathcal{O}(\delta)$. Hence, given that the part of the effective potential not associated with ΔW had a minimum at $\vec{\phi} = \vec{v}(s)$ where $s \in \{-1, 0, 1\}$ parameterizes the \mathbb{Z}_3 fundamental representation elements and $b_j|_{\vec{v}(0)} = 0$ is the singlet element, the energy shift due to ΔW to $\mathcal{O}(\delta)$ is

$$\Delta\rho(s) \equiv \sum_i \Delta V_i|_{\vec{v}(s)} = \sum_i \sum_k \sum_m c_{km}^i P_k(\{v_j \cos\left(\frac{s2\pi}{3}\right)\}) S_m(\{v_j \sin\left(\frac{s2\pi}{3}\right)\}), \quad (\text{D10})$$

Note that $\Delta\rho(1) = \Delta\rho(-1)$. Hence, we only need to determine whether $\Delta\rho(1) - \Delta\rho(0) > 0$ to see if CP singlet has the lowest energy. Since $c_{km}^i \propto \text{sgn}\Delta W$, we can simply flip the sign of $\Delta\rho(1) - \Delta\rho(0)$ by flipping the sign of ΔW if the original choice of sign gives $\Delta\rho(1) - \Delta\rho(0) < 0$. Of course, all of this is under the assumption that the potential is not destabilized by the non-renormalizable operators such that the smallness of the perturbation order δ is meaningful. Stability is generic if the nonrenormalizable terms are dominated by the perturbations in the superpotential since the superpotential contribution is positive definite.

-
- [1] J. R. Ellis, J. F. Gunion, H. E. Haber, L. Roszkowski and F. Zwirner, ‘‘Higgs Bosons in a Nonminimal Supersymmetric Model,’’ *Phys. Rev. D* **39**, 844 (1989).
 - [2] D. E. Lopez-Fogliani and C. Munoz, ‘‘Proposal for a new minimal supersymmetric standard model,’’ *Phys. Rev. Lett.* **97**, 041801 (2006) [arXiv:hep-ph/0508297].
 - [3] N. Escudero, D. E. Lopez-Fogliani, C. Munoz and R. R. de Austri, ‘‘Analysis of the parameter space and spectrum of the $\mu\nu\text{SSM}$,’’ *JHEP* **0812**, 099 (2008) [arXiv:0810.1507 [hep-ph]].
 - [4] V. A. Kuzmin, V. A. Rubakov and M. E. Shaposhnikov, ‘‘On The Anomalous Electroweak Baryon Number Nonconservation In The Early’’
 - [5] A. I. Bochkarev, S. V. Kuzmin and M. E. Shaposhnikov, ‘‘On the Model Dependence of the Cosmological Upper Bound on the Higgs Boson and Top Quark Masses,’’ *Phys. Rev. D* **43**, 369 (1991).
 - [6] M. Pietroni, ‘‘The Electroweak phase transition in a nonminimal supersymmetric model,’’ *Nucl. Phys. B* **402**, 27 (1993) [arXiv:hep-ph/9207227].
 - [7] A. T. Davies, C. D. Froggatt and R. G. Moorhouse, ‘‘Electroweak Baryogenesis in the Next to Minimal Supersymmetric Model,’’ *Phys. Lett. B* **372**, 88 (1996) [arXiv:hep-ph/9603388].

- [8] S. A. Abel, S. Sarkar and P. L. White, “On the Cosmological Domain Wall Problem for the Minimally Extended Supersymmetric Standard Model,” Nucl. Phys. B **454**, 663 (1995) [arXiv:hep-ph/9506359].
- [9] S. A. Abel, “Destabilising divergences in the NMSSM,” Nucl. Phys. B **480**, 55 (1996) [arXiv:hep-ph/9609323].
- [10] C. Panagiotakopoulos and K. Tamvakis, “Stabilized NMSSM without domain walls,” Phys. Lett. B **446**, 224 (1999) [arXiv:hep-ph/9809475].
- [11] S. J. Huber and M. G. Schmidt, “Electroweak baryogenesis: Concrete in a SUSY model with a gauge singlet,” Nucl. Phys. B **606**, 183 (2001) [arXiv:hep-ph/0003122].
- [12] A. Menon, D. E. Morrissey and C. E. M. Wagner, “Electroweak baryogenesis and dark matter in the nMSSM,” Phys. Rev. D **70**, 035005 (2004) [arXiv:hep-ph/0404184].
- [13] S. Profumo, M. J. Ramsey-Musolf and G. Shaughnessy, “Singlet Higgs Phenomenology and the Electroweak Phase Transition,” JHEP **08**, 010 (2007) [arXiv:hep-ph/0705.2425]
- [14] D. J. . Miller, R. Nevzorov and P. M. Zerwas, “The Higgs sector of the next-to-minimal supersymmetric standard model,” Nucl. Phys. B **681**, 3 (2004) [arXiv:hep-ph/0304049].
- [15] P. J. Steinhardt, “Relativistic Detonation Waves And Bubble Growth In False Vacuum Decay,” Phys. Rev. D **25**, 2074 (1982).
- [16] E. Witten, “Cosmic Separation Of Phases,” Phys. Rev. D **30**, 272 (1984).
- [17] A. Kosowsky, M. S. Turner and R. Watkins, “Gravitational Radiation From Colliding Vacuum Bubbles,” Phys. Rev. D **45**, 4514 (1992).
- [18] A. Kosowsky, M. S. Turner and R. Watkins, “Gravitational waves from first order cosmological phase transitions,” Phys. Rev. Lett. **69**, 2026 (1992).
- [19] M. Kamionkowski, A. Kosowsky and M. S. Turner, “Gravitational radiation from first order phase transitions,” Phys. Rev. D **49**, 2837 (1994) [arXiv:astro-ph/9310044].
- [20] R. Apreda, M. Maggiore, A. Nicolis and A. Riotto, “Gravitational waves from electroweak phase transitions,” Nucl. Phys. B **631**, 342 (2002) [arXiv:gr-qc/0107033].
- [21] A. Kosowsky, A. Mack and T. Kahniashvili, “Gravitational radiation from cosmological turbulence,” Phys. Rev. D **66**, 024030 (2002) [arXiv:astro-ph/0111483].
- [22] A. D. Dolgov, D. Grasso and A. Nicolis, “Relic backgrounds of gravitational waves from cosmic turbulence,” Phys. Rev. D **66**, 103505 (2002) [arXiv:astro-ph/0206461].
- [23] A. Nicolis, “Relic gravitational waves from colliding bubbles and cosmic turbulence,” Class. Quant. Grav. **21**, L27 (2004) [arXiv:gr-qc/0303084].
- [24] C. Caprini and R. Durrer, “Gravitational waves from stochastic relativistic sources: Primordial turbulence and magnetic fields,” Phys. Rev. D **74**, 063521 (2006) [arXiv:astro-ph/0603476].
- [25] C. Grojean and G. Servant, “Gravitational Waves from Phase Transitions at the Electroweak Scale and Beyond,” Phys. Rev. D **75**, 043507 (2007) [arXiv:hep-ph/0607107].
- [26] L. Randall and G. Servant, “Gravitational Waves from Warped Spacetime,” JHEP **0705**, 054 (2007) [arXiv:hep-ph/0607158].
- [27] G. Gogoberidze, T. Kahniashvili and A. Kosowsky, Phys. Rev. D **76**, 083002 (2007) [arXiv:0705.1733 [astro-ph]].
- [28] S. J. Huber and T. Konstandin, “Production of Gravitational Waves in the nMSSM,” JCAP **0805**, 017 (2008) [arXiv:0709.2091 [hep-ph]].
- [29] C. Caprini, R. Durrer and G. Servant, “Gravitational wave generation from bubble collisions in first-order phase transitions: an analytic approach,” Phys. Rev. D **77**, 124015 (2008) [arXiv:0711.2593 [astro-ph]].

- [30] A. Megevand, “Gravitational waves from deflagration bubbles in first-order phase transitions,” *Phys. Rev. D* **78**, 084003 (2008) [arXiv:0804.0391 [astro-ph]].
- [31] S. J. Huber and T. Konstandin, “Gravitational Wave Production by Collisions: More Bubbles,” *JCAP* **0809**, 022 (2008) [arXiv:0806.1828 [hep-ph]].
- [32] J. R. Espinosa, T. Konstandin, J. M. No and M. Quiros, “Some Cosmological Implications of Hidden Sectors,” *Phys. Rev. D* **78**, 123528 (2008) [arXiv:0809.3215 [hep-ph]].
- [33] C. Caprini, R. Durrer, T. Konstandin, G. Servant, R. Durrer, T. Konstandin and G. Servant, “General Properties of the Gravitational Wave Spectrum from Phase Transitions,” *Phys. Rev. D* **79**, 083519 (2009) [arXiv:0901.1661 [astro-ph]].
- [34] C. Caprini, R. Durrer and G. Servant, “The stochastic gravitational wave background from turbulence and magnetic fields generated by a first-order phase transition,” arXiv:0909.0622 [astro-ph.CO].
- [35] A. Kusenko, A. Mazumdar and T. Multamaki, “Gravitational waves from the fragmentation of a supersymmetric condensate,” *Phys. Rev. D* **79**, 124034 (2009) [arXiv:0902.2197 [astro-ph.CO]].
- [36] A. Megevand and A. D. Sanchez, “Detonations and deflagrations in cosmological phase transitions,” *Nucl. Phys. B* **820**, 47 (2009) [arXiv:0904.1753 [hep-ph]].
- [37] A. Ashoorioon and T. Konstandin, “Strong electroweak phase transitions without collider traces,” *JHEP* **0907**, 086 (2009) [arXiv:0904.0353 [hep-ph]].
- [38] S. Das, P. J. Fox, A. Kumar and N. Weiner, “The Dark Side of the Electroweak Phase Transition,” arXiv:0910.1262 [hep-ph].
- [39] T. Kahniashvili, L. Kisslinger and T. Stevens, “Gravitational Radiation Generated by Magnetic Fields in Cosmological Phase Transitions,” *Phys. Rev. D* **81**, 023004 (2010) [arXiv:0905.0643 [astro-ph.CO]].
- [40] J. Kehayias and S. Profumo, “Semi-Analytic Calculation of the Gravitational Wave Signal From the Electroweak Phase Transition for General Quartic Scalar Effective Potentials,” *JCAP* **1003**, 003 (2010) [arXiv:0911.0687 [hep-ph]].
- [41] R. Durrer, “Gravitational waves from cosmological phase transitions,” arXiv:1002.1389 [astro-ph.CO].
- [42] D. J. H. Chung and P. Zhou, “Gravity Waves as a Probe of Hubble Expansion Rate During An Electroweak Scale Phase Transition,” arXiv:1003.2462 [astro-ph.CO].
- [43] S. Coleman and E. Weinberg, “Radiative Corrections as the Origin of Spontaneous Symmetry Breaking,” *Phys. Rev. D* **7** 1888 (1973)
- [44] L. Dolan and R. Jackiw, “Symmetry Behavior At Finite Temperature,” *Phys. Rev. D* **9**, 3320 (1974).
- [45] A. Masiero and J.W.F Valle, “A Model for Spontaneous R Parity Breaking,” *Phys. Lett.* **B251** (1990) 273
- [46] F. R. Klinkhamer and N. S. Manton, “A Saddle Point Solution in the Weinberg-Salam Theory,” *Phys. Rev. D* **30**, 2212 (1984).
- [47] Y. Brihaye and J. Kunz, “Electroweak bubbles and sphalerons,” *Phys. Rev. D* **48**, 3884 (1993).
- [48] C. Amsler et al. (Particle Data Group), *Phys. Lett.* **B667**, 1 (2008).
- [49] A. Vilenkin, “Cosmic Strings And Domain Walls,” *Phys. Rept.* **121** (1985) 263.
- [50] J. R. Ellis, K. Enqvist, D. V. Nanopoulos, K. A. Olive, M. Quiros and F. Zwirner, “PROBLEMS FOR (2,0) COMPACTIFICATIONS,” *Phys. Lett. B* **176** (1986) 403.
- [51] G. B. Gelmini, M. Gleiser and E. W. Kolb, “Cosmology of Biased Discrete Symmetry Break-

- ing,” Phys. Rev. D **39** (1989) 1558.
- [52] B. Rai and G. Senjanovic, “Gravity and domain wall problem,” Phys. Rev. D **49** (1994) 2729 [arXiv:hep-ph/9301240].
- [53] S. A. Abel and P. L. White, “Baryogenesis from domain walls in the next-to-minimal supersymmetric standard model,” Phys. Rev. D **52** (1995) 4371 [arXiv:hep-ph/9505241].
- [54] M. E. Carrington, “The Effective potential at finite temperature in the Standard Model” Phys. Rev. D **45** (1992) 2933